Toxoplasma gondii Toc75 functions in import of stromal but not peripheral apicoplast proteins

Lilach Sheiner[1,2], Justin D. Fellows[1], Jana Ovciarikova[2], Carrie F. Brooks[1], Swati Agrawal[1], Zachary C. Holmes[1], Irine Bietz[3], Nadine Flinner[4], Sabrina Heiny[3], Oliver Mirus[4], Jude M. Przyborski[3] and Boris Striepen[1]

[1] Center for Tropical and Emerging Global Diseases & Department of Cellular Biology, University of Georgia, 500 D.W. Brooks Drive, Athens, GA 30602, USA

[2] Wellcome Trust Centre For Molecular Parasitology, Institute of Infection, Immunity & Inflammation, College of Medical, Veterinary & Life Sciences, Sir Graeme Davies Building, University of Glasgow, 120 University Place, Glasgow G12 8TA

[3] Department of Parasitology, Faculty of Biology, Philipps University Marburg, Marburg, Germany

[4] Molecular Cell Biology of Plants, Biocenter N200, 3. OG, Max-von-Laue-Str. 9, 60438 Frankfurt

Running title: *Toxoplasma* Toc75 in apicoplast protein import

Keywords: Omp85, Toc75, Sam50, *Toxoplasma*, *Plasmodium*, Apicomplexa, protein trafficking, apicoplast, complex plastid.

Corresponding author:
Lilach Sheiner. Wellcome Trust Centre For Molecular Parasitology, University of Glasgow, 120 University Place, Glasgow G12 8TA. Phone: +44(0) 141 330 4797 Lilach.Sheiner@glasgow.ac.uk

Synopsis: Protein targeting to plastids and mitochondria of parasites relies on an elaborate system of signals and machinery. We describe *Toxoplasma* and *Plasmodium* Toc75 and Sam50 proteins. TgToc75 is found to mediate stromal but not peripheral apicoplast protein import and to be essential for parasite growth and plastid maintenance

Abbreviations: ATc (Anhydrous tetracycline), POTRA (polypeptide-transport-associated), OMP85 (outer membrane proteins of 85kDa), TIC/TOC (translocons of the inner/outer chloroplast membrane), SIMM (second innermost membrane), PPC (periplastid compartment), Sam50 (sorting and assembly machinery of 50kDa).

Toxoplasma gondii Toc75 functions in import of stromal but not peripheral apicoplast proteins

Lilach Sheiner[1,2], Justin D. Fellows[1], Carrie F. Brooks[1], Swati Agrawal[1], Zachary C. Holmes[1], Irine Bietz[3], Nadine Flinner[4], Sabrina Heiny[3], Oliver Mirus[4], Jude M. Przyborski[3] and Boris Striepen[1]

[1] Center for Tropical and Emerging Global Diseases & Department of Cellular Biology, University of Georgia, 500 D.W. Brooks Drive, Athens, GA 30602, USA

[2] Wellcome Trust Centre For Molecular Parasitology, Institute of Infection, Immunity & Inflammation, College of Medical, Veterinary & Life Sciences, Sir Graeme Davies Building, University of Glasgow, 120 University Place, Glasgow G12 8TA

[3] Department of Parasitology, Faculty of Biology, Philipps University Marburg, Marburg, Germany

[4] Molecular Cell Biology of Plants, Biocenter N200, 3. OG, Max-von-Laue-Str. 9, 60438 Frankfurt

Correspondence: Lilach.Sheiner@glasgow.ac.uk

Running title: *Toxoplasma* Toc75 in apicoplast protein import

Keywords: Omp85, Toc75, Sam50, *Toxoplasma*, *Plasmodium*, Apicomplexa, protein trafficking, apicoplast, complex plastid.

Abstract

Apicomplexa are unicellular parasites causing important human and animal diseases, including malaria and toxoplasmosis. Most of these pathogens possess a relict but essential plastid, the apicoplast. The apicoplast was acquired by secondary endosymbiosis between a red alga and a flagellated eukaryotic protist. As a result the apicoplast is surrounded by four membranes. This complex structure necessitates a system of transport signals and translocons allowing nuclear encoded proteins to find their way to specific apicoplast sub-compartments. Previous studies identified translocons traversing two of the four apicoplast membranes. Here we provide functional support for the role of an apicomplexan Toc75 homolog in apicoplast protein transport. We identify two apicomplexan genes encoding Toc75 and Sam50, both members of the Omp85 protein superfamily. We localize the respective proteins to the apicoplast and the mitochondrion of *Toxoplasma* and *Plasmodium*. We show that the *Toxoplasma* Toc75 is essential for parasite growth and that its depletion results in a rapid defect in the import of apicoplast stromal proteins while the import of proteins of the outer compartments is affected only as the secondary consequence of organelle loss. These observations along with the homology of the protein to chloroplast Toc75 suggest a role in transport through the second innermost membrane.

Introduction

Apicomplexan parasites are the cause of important human and animal diseases, including malaria and toxoplasmosis. Most of these pathogens possess a relict plastid named the apicoplast. While the apicoplast is no longer photosynthetic, it has important metabolic roles and supplies the parasite with fatty acids, isoprenoids, and heme (1, 2). The apicoplast is the product of secondary endosymbiosis whereby a single celled red alga was engulfed by a flagellated eukaryote and a stable endosymbiotic relation ensued. This event gave rise to a large and diverse group of photosynthetic and non-photosynthetic eukaryotes referred to by some authors as the chromalveolates (3, 4). The apicoplast and the plastids of other chromalveolates are surrounded by four membranes reflecting their complex endosymbiotic origin. The innermost membrane and second innermost membrane (SIMM) originate from the algal primary plastid. The next membrane out, bounding the periplastid compartment, originates from the algal plasma-membrane and the outermost membrane is believed to be derived from the host endomembrane system (reviewed in (5)).

Key to the conversion of the algal endosymbiont into a plastid was the transfer of the symbiont's genes to the nucleus of the host, allowing far reaching transcriptional and translational control by the host. This transfer of genetic material from the endosymbiont to the host is only possible upon coevolving systems that allow the import of host-translated proteins into the endosymbiont. In the case of the apicoplast this requires translocation across its four delineating membranes to reach the

stroma. Apicomplexan parasites target large numbers of nuclear encoded proteins to the apicoplast. 10% of the *Plasmodium falciparum* proteome is predicted to be transported to the apicoplast, underscoring the importance of this trafficking pathway (6). Our current model (Figure 1A) assumes this pathway to start with signal sequence guided entry into the ER lumen, likely via the Sec61 translocon. Trafficking from the ER to and across the outer apicoplast membrane remains poorly understood, but potentially depends on signals typically involved in endocytosis or autophagy (7-9) and may take place by more than one route (10, 11). Translocation across the periplastid membrane is mediated by machinery evolved from the endosymbiont's ER-associated protein degradation (ERAD) system (12-16). Finally, based on their evolutionary origin in chloroplast membranes, it is believed that homologs of the translocons of the inner and outer chloroplast membrane (TIC/TOC) function in translocation of proteins through the apicoplast's two innermost membranes. Experimental evidence supports the role of the TIC complex in apicoplast protein import (17, 18) but is lacking in the case of the putative TOC machinery.

Most stromal proteins possess a bipartite signal, comprised of a signal and a transit peptide (6). Upon translocation to the ER lumen the N-terminal signal peptide portion of the leader is cleaved off, exposing the transit peptide that is required for further trafficking (19). In diatoms, a group likely descended from the same endosymbiotic event as Apicomplexa, subplastidal targeting depends on the first amino acid (position +1) of the transit peptide (20, 21). An aromatic amino acid at this position targets the protein through the SIMM *en route* to the stroma; otherwise, the proteins are retained in the periplastid space. Incidentally, an aromatic residue is also required for import through the outer membrane of primary plastids of red algae (20, 22, 23) and of glaucocystophytes (24). In the primary plastids of glaucocystophytes, recognition of the aromatic residue depends on an Omp85 family protein that functions as the translocation pore of their primitive TOC machinery (25).
Abundance of aromatic residues at position +1 was reported for the transit peptides of additional Chromalveolates (26, 27). These studies include *Toxoplasma* and *Plasmodium* spp where enrichment of phenylalanine was reported at this position (27). Nevertheless the role of this amino acid was so far not supported experimentally. The targeting sequence of a *Toxoplasma* apicoplast stromal protein, ferredoxin-NADP+ reductase (FNR), was studied in detail (28). An extensive series of deletions within the N-terminal sequence suggested the presence of redundant signals and did not implicate a particular residue at position +1 (28). Whether this is true for all apicoplast stromal proteins remains unknown.

Omp85 (for outer membrane protein of 85 KDa) is a protein that catalyzes insertion and assembly of β-barrel proteins into the outer membrane of gram-negative bacteria. The more widely distributed superfamily of Omp85-related proteins shares a conserved domain organization that includes N-terminal polypeptide-transport-associated (POTRA) repeats and a C-terminal transmembrane β-barrel. Three main eukaryotic representatives are well described: the mitochondrial sorting and assembly machinery of 50 kDa (Sam50/Tob55) and the chloroplast proteins Toc75-III and Toc75-V (29, 30). Like its bacterial ancestor, Sam50/Tob55 recognizes mitochondrial outer membrane proteins in the intermembrane space after they fully translocate across the outer membrane and catalyzes their insertion into it (31, 32). Toc75V (or Oep80 for outer envelope protein 80) is hypothesized to perform a similar role in the outer chloroplast membrane (33-35). Toc75III functions as the channel of the TOC translocon in the outer chloroplast membrane that allows proteins to fully translocate through it (36).
In diatoms, an Omp85-like protein, *Pt*Omp85, was identified that possesses a bipartite plastid targeting signal and two POTRA domains (37). This protein is localized to the diatom complex plastid and both its N and C terminal domain face the periplastid compartment (37). Using the sequence of *Pt*Omp85, Bullmann and co-workers were able to identify putative apicomplexan homologs (37, 38), and this assignment gained further support from Hirakawa and coworkers (39). These homologs possess features supporting their Omp85 affiliation such as a signal sequence, the typical N-terminal POTRA signature, and a C-terminus that likely forms a beta-barrel. However, their putative role in apicoplast protein import has not been evaluated experimentally.
Here we seek to gain new insights into the pathways by which apicoplast proteins traverse the SIMM. We analyze the targeting sequences of a large group of experimentally confirmed apicoplast proteins (summarized in (40)), to assess the abundance of an aromatic residue that may be recognized by an Omp85. We confirm the identity and localization of Omp85 proteins from both *Plasmodium falciparum* and *Toxoplasma gondii* and demonstrate that the *Toxoplasma* Toc75 functions in the import of proteins into the stroma of the apicoplast. Finally, we show that import of peripheral apicoplast protein is not dependent on TgToc75 activity, which is consistent with the potential assignment of TgToc75 to the second innermost of the four apicoplast membranes.

Results

Sequence analysis reveals moderate enrichment of aromatic residues at position +1

of stromal proteins and the presence of two omp85-like proteins in apicomplexan genomes

We used sequence analysis to identify signals and machinery potentially involved in traversal of the apicoplast SIMM membrane. We have recently substantially expanded the repertoire of experimentally confirmed apicoplast proteins in *Toxoplasma gondii* (40) now counting 47 proteins (Table S1). We utilized the online prediction algorithm SignalP (http://www.cbs.dtu.dk/services/SignalP-3.0/) to predict the signal peptide cleavage site of all 47 proteins. Using SignalP 3.0 server we were able to define with high certainty the amino acid at position +1 of the transit peptide of 29 of these proteins (Table S1 shows the predictions obtained with both SignalP servers: 3.0 and 4.1). Figure 1B shows the distribution of +1 residue abundance in (i) 22 stromal and (ii) 7 peripheral proteins. We found that 27% of stromal proteins have an aromatic residue (mostly a phenylalanine) at the predicted position +1 while none of the non-stromal proteins feature an aromatic amino acid at this position (Table S1, Figure 1B).

Next, we revisited the repertoire of potential apicomplexan Omp85-like encoding genes. Using jackhmmer to mine the NCBI non-redundant database, and subsequent reciprocal BLAST searches against the EupathDB, we identified two Omp85-like proteins in *T. gondii* (TGME49_205570, TGME49_272390), *P. falciparum* (PF3D7_0608310, PF3D7_1234600), and several other apicomplexan species (Table 1).
To determine the respective affiliation of these genes, we selected representative species across the eukaryotic tree of life and reconstructed a majority rule consensus tree from 1,000 bootstrap trees (Figure 2; see also maximum likelihood tree Figure S1A). The tree shows a clear split into Sam50 and Toc75 clades supported by a bootstrap of 100. We classified sequences TGME49_205570 and PF3D7_0608310 as Sam50 (herein named TgSam50 and PfSam50, respectively) and sequence TGME49_272390 as Toc75 (named TgToc75). PF3D7_1234600 could not be resolved with certainty in this analysis, and thus was not included in the reconstruction of this tree, however subsequent analysis included PF3D7_1234600 (Figure S1B) and used the POTRA region only (Figure S1C) to construct a maximum likelihood tree which shows that PF3D7_1234600 is affiliated with the Toc75 homologs from Chromalveolates (herein named PfToc75). The presence of two POTRA domains in PfToc75 and TgToc75 and a predicted apicoplast targeting signal in PfToc75 support this affiliation.

Mutagenesis of a phenylalanine at position +1 of the transit peptide of the stromal protein ACP to alanine results in peripheral retention

The putative role of the aromatic residue at position +1 of the stromal protein ACP in trafficking was analyzed via mutagenesis. YFP-tagged ACP with the wild type sequence (ACP_{WT}YFP) and YFP-tagged ACP with the phenylalanine replaced to an alanine ($ACP_{F/A}$YFP) were transiently transfected and their localization was assessed by high-resolution microscopy. While ACP_{WT}YFP showed precise co-localization with the stromal marker CPN60 (12), $ACP_{F/A}$YFP showed very little overlap with it (Figure 1C). Similarly, the signal from ACP_{WT}YFP did not overlap with signal from the HA-tagged periplastid marker ATrx2 (40), while $ACP_{F/A}$YFP showed substantial co-localization with this periplastid marker (Figure 1C).
The signal peptide cleavage prediction by SignalP 3.0 differs from that obtained by SignalP 4.1. While both suggest the phenylalanine at position +1 with high likelihood, the latter predicts an upstream tyrosine to be at this position. We generated YFP-tagged ACP with the tyrosine replaced to an alanine ($ACP_{Y/A}$YFP) and examined its localization upon transient expression by high-resolution microscopy. Similar to ACP_{WT}YFP, $ACP_{Y/A}$YFP showed full co-localization with the stromal marker CPN60 and little overlap with the periplastid marker ATrx2 (Figure 1C).

Localization of the T. gondii and P. falciparum Omp85 proteins to the apicoplast and mitochondrion supports their assignments as Toc75 and Sam50

The assignment of Omp85 proteins to their respective families as determined by the phylogeny was tested by localization studies. Both the first 78, and the first 95 N-terminal amino acids derived from both TgToc75 (Figure S2) and PfToc75 (Figure 3A) target to a punctate structure within the parasite that co-localized with the *Toxoplasma* or *Plasmodium* apicoplast markers FNR-RFP or ACP respectively. We conclude that these N-termini serve in apicoplast localization of these proteins. Moreover, full-length TgToc75 also co-localizes with the apicoplast marker FNR-RFP further supporting the Toc75 affiliation (Figure 3A). High resolution microscopy and co-staining with the stromal marker CPN60 suggested TgToc75 localization is peripheral to the apicoplast stroma (Figure 3B). In line with the expected peripheral localization of a Toc75 homolog.
We next assessed the localization of the second Omp85 homologue identified in each of the species. A mitochondrial targeting signal was predicted for PfSam50 but not for TgSam50 (Table S1). The first 60 amino acids of PfSam50 targeted GFP to a ribbon-like structure within *P. falciparum* parasites that co-localized with the signal obtained through the use of MitoTracker (Figure 3C). Likewise, full-length TgSam50 co-localized with the mitochondrial marker Hsp60-RFP (Figure 3C).

Finally, co-transfection of both full-length HA-tagged TgToc75 and full-length Ty-tagged TgSam50 in *T. gondii* reveals two distinct patterns of fluorescence with minimal signal overlap. This demonstrates the existence of two Omp85-like proteins in *T. gondii* in the two distinct endosymbiotic compartments; the apicoplast and the mitochondrion (Figure 3D). Taken together, our localization experiments are entirely consistent with the classification proposed by phylogenetic analysis.

TgToc75 is required for parasite growth and apicoplast maintenance

To test whether TgToc75 functions in apicoplast protein import we generated a mutant in which its expression level can be manipulated. First we constructed the *TATiΔKu80iToc75pi* line: in this parasite the TgToc75 open reading frame is separated from its native promoter by a tetracycline-regulatable promoter cassette (40). This parasite line was established using cosmid (PSBL491) recombineering (41, 42) (Figure S3). Our analysis of this line suggested that TgToc75 is essential for parasite growth (Figure S3), and that its down regulation results in apicoplast demise and in a stromal protein modification defect (Figure S3), as expected from interference in the apicoplast protein import machinery (12, 18, 40). However, this mutant proved unstable resulting in loss of regulation. We thus utilized recombineering to construct the *TATiΔKu80iToc75pr* line: in this line we replaced the TgToc75 native promoter with the tetracycline-regulatable promoter cassette (Figure 4A). This line is stable and was used for the remainder of the analyses. We found down regulation of TgToc75 (Figure 4B) to result in a growth defect as observed by plaque assay (Figure 4C). Additionally, TgToc75 depletion resulted in loss of the apicoplast evident by loss of plastid DNA, which was quantified via quantitative PCR, as well as by loss of immunofluorescence staining of the apicoplast stromal protein CPN60 (Figure 4D, E). Organelle loss was gradual starting with 28% loss at 24 hours of Toc75 down regulation and reaching 99.5% loss by 96 hours.

Loss of TgToc75 results in loss of import with more rapid impact on stromal when compared to peripheral apicoplast proteins

To examine apicoplast protein import under TgToc75 down regulation we followed the maturation of the plastid stromal protein ACP (12, 17, 18, 40). Typically two bands can be observed for this protein by Western blot, a larger precursor protein *en route* to the plastid, and a mature protein lacking the leader peptide due to the activity of stromal signal peptidase (18, 19, 43, 44). By following endogenously tagged ACP (40) we detected accumulation of un-cleaved precursor starting at 48 hours after Toc75 down regulation (Figure 5A). Interestingly, the precursor of the protein encoded by TGME49_001270, an outer apicoplast membrane protein (40), does not accumulate even as late as 72 hours (Figure 5B). To assess whether this difference is specific to TgToc75 depletion we conducted control experiments with a regulated mutant of the periplastid protein 1 (PPP1). PPP1 is a periplastid compartment resident protein that plays an essential role in apicoplast protein import and it is likely required for the translocation of proteins across the periplastid membrane (40). Here we show that upon down regulation of PPP1 both the stromal ACP and the outer membrane protein encoded by TGME49_001270 show precursor accumulation ((40) and Figure 5C,D). We conclude that proteins pass through the PPP1 associated translocon first and the Toc75 translocon second and that the outer translocon can act and assemble (at least for a limited time) independently of Toc75.

To test whether these observations hold true for other stromal and non-stromal proteins we examined two additional markers, the stromal protein LytB (45) and the periplastid protein PPP1. In order to follow protein maturation in real time we measured maturation of LytB and PPP1 expressed transiently at different time points after TgToc75 down regulation. In agreement with the above observations, newly synthesized stromal LytB, shows precursor accumulation starting as early as 24 hours after TgToc75 down regulation (Figure 5E), while the newly synthesized periplastid protein PPP1 shows precursor accumulation only late into suppression (72 hours, Figure 5F) when many apicoplasts are lost due to secondary effects (Figure 4D, E).

Discussion

The acquisition of secondary plastids went hand in hand with the development of appropriate machineries for protein import (3). The complex nature of these plastids requires a set of signals allowing precursor protein trafficking to their final sub-organellar destination. An elevated abundance of aromatic amino acids, particularly phenylalanine, at position +1 downstream of the predicted signal peptide cleavage site, was reported in several chromalveolates and was proposed to be a functional feature of the transit peptide in these organisms (26, 27). An aromatic signature residue, most frequently a phenylalanine (but also tyrosine and tryptophan), at position +1 of the transit peptide, was proposed to serve as forward signaling from the periplastid space through the two innermost membranes in several groups or organisms with secondary plastids. A similar requirement is found for import into the primary plastids of red algae (20, 22, 23, 46). Gould and coworkers suggested a model according to which all proteins targeted to a complex plastid of red origin gain entry to the periplastid

compartment by a common indiscriminate mechanism (46). We analyzed 47 *T. gondii* sequences of proteins experimentally shown to target to the apicoplast periphery or the apicoplast stroma. Of those we could assess 29 proteins with high certainty. This analysis does not align with the notion of a uniform mechanism. On one hand we show enrichment of an aromatic residue at position +1 in the putative transit peptides of proteins that cross all 4 apicoplast membranes (Table S1, Figure 1B). Further, our mutagenesis experiments support the idea that this aromatic +1 residue plays a role in the targeting of the stromal ACP (Figure 1C). However, on the other hand, not all stromal proteins obey this rule. In fact, the majority (73%) of stromal proteins were not predicted to have a +1 aromatic residue, suggesting alternative signals may be involved in SIMM traversal. Indeed, in the case of FNR, for which most computational analyzes ((28) + TableS1) do not predict an aromatic residue at position +1, other signals were implicated in stromal localization (28). We also observed the lack of aromatic residues at position +1 of peripheral proteins, however the repertoire of well documented residents of these outer compartments is still limited (only 7 predicted with confidence). Overall our observations are consistent with the previously proposed (20,21,27) broader conservation of the +1 aromatic signal as one of the mechanisms for stromal import but also suggest alternative, yet to be characterized, signals in Apicomplexa.

The secondary plastid of Apicomplexa and related taxa was shaped by contributions from three organisms: a cyanobacterium, a red alga and a flagellated heterotrophic eukaryote. The current model of protein import suggests that each membrane is traversed with the help of machinery derived from its organism of origin. This model gradually gained support with the identification and functional characterization of TIC components (17, 18) and of ERAD/SELMA components (12, 13, 16). The confirmation of the TOC link in this model was slow to emerge, most likely due to significant primary sequence divergence of the TOC components in organisms with complex plastids. An important breakthrough was made by the identification of an Omp85-like protein in the diatom *Phaeodactylum tricornutum,* for which phylogeny, subcellular localization and electrophysiology support affiliation with Toc75 (37). Here we provide experimental support for the general conservation of this transport pathway by localization of the apicomplexan homologs of PtToc75 to the apicoplast (Figure 3) and by functional analysis of TgToc75 (Figure 4 and 5).

Aside from TgToc75/PfToc75, our search for members of the polypeptide-transporting β-barrel protein superfamily in the genomes of Apicomplexa identified only one additional gene in each species, which encodes a Sam50/Tob55 homolog. We supported this assignment by localizing these proteins to the mitochondrion (Figure 3B). TgToc75/PfToc75 thus likely represent the only plastid Omp85s in these parasites, an observation that joins a growing line of evidence for a single Toc75 in the red lineage of plastids. The genome of the red alga *C. merolae* encodes a single Toc75 (47). Bullmann and coworkers similarly report a single Toc75 in their analysis of the genomes of the diatoms *P. tricornutum* and *Thalassiosira pseudonana,* and the haptophyte *Emiliania huxleyi* (37). In contrast, higher plants possess two functional Toc75 homologs: Toc75V/Oep80, which mediates assembly of proteins into the outer membrane of the chloroplast (35), and Toc75-III (36), which is the central component of the TOC machinery. At least two plastidial Toc75 proteins were identified in other members of the green lineage, and in all cases at least one ortholog of Toc75V/Oep85 was identified (39, 47). Whether the Toc75 found in the red lineage serves the roles of both of its green algal counterparts is unclear at this point.

Others (37) and we herein hypothesize that TgToc75 plays a role in precursor transit through the SIMM. To test TgToc75's involvement in apicoplast protein import we generated a conditional *TgToc75* mutant parasite cell using our recently described tetracycline-based promoter replacement system (40). We demonstrated *TgToc75* to be a firm requirement for apicoplast protein import, apicoplast maintenance, and parasite growth consistent with the hypothesis that this protein is an essential component of the apicoplast protein import machinery.

In agreement with a role for TgToc75 in stromal protein import, we observed a defect in precursor processing for the endogenously YFP-tagged stromal protein ACP (Figure 5A). The slow onset of this defect may reflect an overall slow impact of Toc75 mutants as previously noted in primary chloroplast (48), or could result from the long half-life of mature ACP as noted before (18, 40). We therefore tested an independent stromal protein (LytB) by transient transfection to follow the protein synthesized at various time points after Toc75 down regulation was ongoing. This assay showed impaired precursor processing as early as 24h after TgToc75 down regulation (Figure 5E) and before secondary defects due to loss of the organelle (Figure 4D,E). Overall the TgToc75 mutant produces a phenotype similar to previously studied inducible mutants in components of the apicoplast protein import machinery (12, 17, 18, 40) supporting the proposed role of TgToc75 in mediating stromal precursor protein import.

Interestingly, unlike the stromal proteins, only a mild processing defect was observed for outer compartment proteins (Figure 5B,F). This is specific to TgToc75 depletion, as processing is blocked for an outer compartment protein upon

disruption of the periplastid import machinery (Figure 5D). These experiments support a model under which proteins of the apicoplast outer compartments (periplastid and outer membrane compartments) are not dependent on TgToc75 for their transport into the organelle while stromal proteins (ACP and LytB) are. Taken together with the phylogenetic analyses these observations support TgToc75 as a component of the apicoplast TOC channel, however direct experimental demonstration for its activity at the SIMM is yet to be established.
Finally, seeing that outer compartment protein processing occurs under depletion of TgToc75, our findings support the previous predictions (15) of the existence of at least two apicoplast transit peptide peptidases: one in the lumen and one in the outer compartments upstream of the TOC machinery.

While we provide functional support for the role of Toc75 in protein import into complex plastids of red origin, we were unable to identify other components of the TOC machinery in the genomes of Apicomplexa by using BLAST searches, in line with previous reports (38, 47). Most striking is the apparent absence of homologs for the receptor components Toc159/Toc120/Toc132 and Toc34/Toc33 (49) that are found in primary plastids of both the green and the red lineage (47, 50). Interestingly, a similar finding was recently reported for the secondary plastid of green origin of *B. natans* (39). Hirakawa and coworkers suggest an explanation whereby unlike primary plastids where the TOC machinery has to distinguish plastid proteins from all other cytoplasmic and mitochondrial proteins, the TOC machinery of secondary plastids interacts with a more focused repertoire of precursors that was already screened by previous translocation machineries. This idea is supported by the observation that transit peptides of secondary plastid apparently lack features that differentiate between mitochondria and plastid targeting in organisms with primary plastids (27). In agreement with this model it was proposed before that in membranes with a primitive, reduced TOC machinery, the Omp85-like component is involved in precursor selection that is based on the presence of an aromatic residue (25). While it is clear that apicoplast stromal import could not be explained by this simple model ((28), TableS1), our finding provides grounds for further investigation of the potential role of such a pathway in the trafficking of at least some of the stromal proteins.

One of the soluble components that interact with the TOC machinery is Tic22 (51). TgTic22 was identified and functionally characterized using a similar genetic system (17). TgTic22 down regulation results in a phenotype similar to our observations here, whereby the maturation of a stromal marker (FNR-DHFR-cMyc) was reduced at 24h after addition of ATc (17), supporting their potential cooperation in a common pathway. Interestingly, Toc75 and Tic22 are the sole TOC components found so far in secondary red plastids. They are also the only TOC components for which a clear homology with their cyanobacterial ancestors was demonstrated (51, 52).

Materials and methods

Search for Omp85 homologs
The non-redundant protein database was downloaded from NCBI (ftp://ftp.ncbi.nlm.nih.gov/blast/db/FASTA/) and screened with jackhmmer (53) using AtToc75-III as query for members of the Omp85 superfamily. Then *Toxoplasma gondii* ME49 and *Plasmodium falciparum* 3D7 genomes were screened (i) with BLAST for homologs of *Toxoplasma* and *Plasmodium* sequences detected by jackhmmer and (ii) with hmmsearch (53) for proteins with at least one of the following PFAM (54) domains: Surface_Ag_VNR (PF07244), Bac_surface_Ag (PF01103), POTRA_2 (PF08479), ShlB (PF03865). Finally the resulting *Plasmodium* and *Toxoplasma* Omp85 homologs were used as query for BLASTs of EupathDB (http://eupathdb.org/eupathdb/) to identify the respective homologs in other Apicomplexan genomes.

Phylogenetic analysis
A multiple sequence consensus alignment was constructed as described in (55) from a subset of Sam50 and Toc75 homologs. From this alignment a maximum likelihood phylogeny was reconstructed with RAxML (56) using the WAG model (57) and gamma-distributed rate heterogeneity. Branch support values were derived from 1,000 rapid bootstrap trees and a majority rule consensus tree was constructed from them. Note that the older gene model for TgToc75, TGME49_072390, predicts a longer protein, which includes the extreme C-terminal part of the β-barrel (missing in the new gene model: TGME49_272390). The alignment and phylogeny were done with the longer older gene model. Similarly, an older gene model of PfSam50, PFF0410w, spans two new predicted genes: PF3D7_0608300/0608310. We experimentally confirmed the older gene model (see supplementary text) new accession numbers were produced for the confirmed sequences (TgToc75 - KT271755; PfSam50 - KT271756). The alignment and phylogeny were performed using the new and shorter version PF3D7_0608310, containing the conserved domain.

Constructs:
Toxoplasma gondii:
Total RNA was extracted from *T. gondii* (strain RH) using Trizol (Invitrogen). Overlapping cDNA fragments encoding the entire TgToc75

and TgSam50 genes were amplified from total RNA using the SuperScript III One-Step RT-PCR kit (Invitrogen) and primers shown in Table S2. All resulting PCR products were cloned using the ZeroBlunt PCR cloning kit (Invitrogen) and sequenced (GATC, Konstanz). TgToc75[78], TgToc75[95]: Fragments encoding the noted amino acids were amplified from cDNA (primers in Table S2), and inserted into the TUB8mycGFPMyoATy *T. gondii* expression vector resulting in expression of these N-terminal amino acids directly fused to a Ty tag. Using EcoRI/NsiI allowed for an in frame C-terminal Ty tag. TgToc75$^{full\text{-}Ty}$: A full-length cDNA version (based on the older gene model - TGME49_072390) of the *TgToc75* gene (removing an internal EcoRI restriction site) was synthesized by Geneart (Regensburg) and cloned into the TUB8mycGFPMyoATy vector as above. TgToc75$^{full\text{-}HA}$: TgToc75$^{full\text{-}Ty}$ was digested with NsiI/PacI and a 3x hemagglutinin (HA) tag was inserted, having been generated by amplification (primers in Table S2). TgSam50$^{full\text{-}HA}$: A full-length cDNA version of the *TgSam50* gene was synthesized by Geneart (Regensburg) and cloned into the TgToc75$^{full\text{-}HA}$ vector using EcoRI/NsiI.

Inducible knock-down cosmids:
pGDT7S4 (42) was used as templates to PCR amplify a 4Kb promoter modification cassette (primers in Table S2) containing a gentamycin resistance marker for selection in bacteria, a DHFR marker for the subsequent selection in *T. gondii* and the T7S4 promoter to be inserted upstream of TgToc75 start site (*pi*) or to replace the TgToc75 endogenous promoter sequence (*pr*). This cassette was used for PSBL491 recombineering as done before (41).

Site directed mutagenesis:
To change the residues at position +1 of the transit peptide of ACP within plasmid pTUB8ACP$_{WT}$YFP, primers ACP$_{F/A}$mutR or ACP$_{Y/A}$mutF/R (Table S2) were used in a site-directed mutagenesis reaction using the commercial QuikChange II Site-Directed Mutagenesis Kit (Stratagen) according to manufacturer's instructions.

Plasmodium falciparum:
Total RNA was extracted from *P. falciparum* (3D7) using Trizol (Invitrogen). PfToc75[78], PfToc[95], PfSam50[60]: Fragments encoding the noted amino acids were amplified from total RNA (primers in Table S2), and inserted into the XhoI/AvrII sites of pARL2-GFP. All final constructs were verified by restriction digest and automated sequencing (GATC, Konstanz).

Cell culture and transfection of T. gondii *and* P. falciparum.
Cultivation and transfections of *T. gondii* (strain RH delta hxgprt, a kind gift of Markus Meissner, and our TATi/ΔKu80strain (40)) in human foreskin fibroblasts and *P. falciparum* (3D7) in human erythrocytes was carried out under standard conditions. *P. falciparum* transfectants were selected with 2.5nM WR99210 (a kind gift of Jacobus Pharmaceuticals). Promoter replacement or insertion in TATi/ΔKu80strain was selected with 1μM Pyrimethamin as described in (42). FNR^{RFP} and Hsp60^{RFP} constructs were a kind gift of Markus Meissner.

Plaque assay
Fresh monolayers of HFF were infected with parasites in the presence or absence of 1.5 μg/ml ATc for 7 days. Fixation, staining and visualization were performed as previously described (40).

RT-PCR and qPCR
RNA was prepared from cultures grown without ATc or with ATc for 24 and 72 hours using RNeasy® (QIAGEN) and reverse transcriptase reaction was performed using SuperScript® III First-Strand Synthesis (Invitrogen) (both according to the manufacturer's instructions). 300ng of the resulting template was used for qPCR reaction using SYBR Green Mix (Bio-Rad) and primers TOC75RTPCRf2 and TOC75RTPCRr2. Copy number control was performed using cosmid PSBL491 as template. Genomic DNA was prepared from cultures grown without ATc or with ATc for 24 and 72 hours using DNeasy® (QIAGEN). 100ng of the resulting template was used for qPCR reaction using SYBR Green Mix (Bio-Rad) and primers Apg-qPCR-F/R for apicoplast and UPRT-qPCR-F/R for nuclear genomes. A copy number control was performed using specific plasmids as described in (58).

IFA and imaging
T. gondii: Immunofluoresence was carried out on infected HFF cells seeded onto glass cover slips. Cells were fixed with 4% paraformaldehyde/PBS (15 min, RT), permeabilised with 0.5% T-X-100/PBS (15 min, RT), blocked with 5% BSA/PBS (30 min, RT), incubated with primary antibodies diluted in 5% BSA/PBS (1h, RT), washed three times in PBS, incubated with suitable fluorescent-conjugated secondary antibodies (1h, RT), washed three times in PBS, incubated with 50 ng/ml Hoechst 33258/PBS (5 min, RT), washed in distilled water and cover slips were mounted onto glass slides using Fluoromount (SouthernBiotech).
P. falciparum: Cells were fixed in 4% Paraformaldehyde/0.00075% Glutaraldehyde (37ºC, 30 min), quenched in 125 mM Glycine/PBS, Hoechst 33258 (Molecular probes) was used at 50ng/ml for fixed parasites or 10 mg/ml for live parasites.
Images were acquired on Carl Zeiss Axio Observer inverse epifluorescence microscope (Figure3, FigureS2). Individual images were imported into ImageJ64 (version 1.46r, available at http://rsb.info.nih.gov/ij), converted to 8-bit greyscale, subjected to background subtraction, and overlaid. Image in FigureS3 was taken using a Delta Vision microscope as described (12). Antibodies and concentrations

used were: rabbit anti-HA (Sigma-Aldrich, 1:50); mouse anti-Ty tag (a kind gift of Keith Gull, 1:20); anti-ACP (a kind gift of Geoff McFadden, 1:500), rabbit anti-CPN60 (1:500), Cy2 goat anti-rabbit, Cy3 goat anti-Rabbit, Cy2 goat anti-mouse, Cy3 goat anti-mouse (all Jackson Immuno Research Laboratories, 1:2000).

For superresolution structural illumination microscopy (SR-SIM), stacks of 30-40 images were taken with increments of 0.091 µm in a Zeiss Elyra Superresolution microscope (Jena, Germany) with a 63x oil immersion objective and an immersion oil with a refractive index of 1.518 (Zeiss, Germany). Superresolution images were generated using ZEN software (version Zen 2012 SP1, Zeiss, Germany) and processed into their final form using FIJI software (59).

Apicoplast protein import assay and Western blot analyses:

Western blot of steady-state levels of proteins: clonal parasite lines grown in the presence or absence of ATc and collected (1500g, 10min, RT), lysed in sample buffer, separated by SDS-PAGE and blotted using anti-GFP (ROCHE) antibody for ACP-YFP and anti-HA antibody (SIGMA) for TGME49_001270.

Western blot of transiently expressed proteins: *TATiΔKu80iToc75pr* parasites were grown in ATc for a given period of time, then transiently transfected with pBT_LytB or pTUB8-PPP1-HA, and let to grow for an additional 24h to reach the total desired time of down-regulation (for example for 72 hours +ATc time point, parasites were grown for 48 hours in ATc, transfected and then grown for an additional 24h in ATc). Transfected and treated parasites were collected, separated by SDS-PAGE and blotted using anti-HA or anti-Ty antibodies.

Pulse/chase analysis was performed as described before (12, 18, 40).

Acknowledgment

This work was supported in part by U.S. National Institutes of Health RO1 grants AI064671, AI084415 (to BS) and K99 grant AI103032 (to LS). BS is a Georgia Research Alliance distinguished investigator. JDF is a predoctoral fellow of the American Heart Association. IB and SH were supported by DFG grant PR1099/2-1 (to JMP). JO was supported by a Wellcome Trust Institutional Strategic Support Fund Fellowship to LS. NF was supported by CEF and SFB807 to Enrico Schleiff and we would like to thank him for critical discussions. JMP and LS wish to thank Markus Meissner for initial assistance with cultivation and transfection of *T. gondii* and for the kind contribution of antibodies and markers.

References

1. Sheiner L, Vaidya AB, McFadden GI. The metabolic roles of the endosymbiotic organelles of *Toxoplasma* and *Plasmodium* spp. Curr Opin Microbiol 2013;16(4):452-458.

2. van Dooren GG, Striepen B. The algal past and parasite present of the apicoplast. Annu Rev Microbiol 2013;67:271-289.

3. Cavalier-Smith T. Principles of protein and lipid targeting in secondary symbiogenesis: euglenoid, dinoflagellate, and sporozoan plastid origins and the eukaryote family tree. J Eukaryot Microbiol 1999;46(4):347-366.

4. Koreny L, Sobotka R, Janouskovec J, Keeling PJ, Obornik M. Tetrapyrrole synthesis of photosynthetic chromerids is likely homologous to the unusual pathway of apicomplexan parasites. Plant Cell 2011;23(9):3454-3462.

5. Sheiner L, Striepen B. Protein sorting in complex plastids. Biochim Biophys Acta 2013;1833(2):352-359.

6. Foth BJ, Ralph SA, Tonkin CJ, Struck NS, Fraunholz M, Roos DS, Cowman AF, McFadden GI. Dissecting apicoplast targeting in the malaria parasite *Plasmodium falciparum*. Science 2003;299(5607):705-708.

7. Jayabalasingham B, Voss C, Ehrenman K, Romano JD, Smith ME, Fidock DA, Bosch J, Coppens I. Characterization of the ATG8-conjugation system in 2 *Plasmodium* species with special focus on the liver stage: possible linkage between the apicoplastic and autophagic systems? Autophagy 2014 ;10(2):269-284.

8. Tawk L, Dubremetz JF, Montcourrier P, Chicanne G, Merezegue F, Richard V, Payrastre B, Meissner M, Vial HJ, Roy C, Wengelnik K, Lebrun M. Phosphatidylinositol 3-monophosphate is involved in *Toxoplasma* apicoplast biogenesis. PLoS Pathog 2011 ;7(2):e1001286.

9. Tomlins AM, Ben-Rached F, Williams RA, Proto WR, Coppens I, Ruch U, Gilberger TW, Coombs GH, Mottram JC, Muller S, Langsley G. *Plasmodium falciparum* ATG8 implicated in both autophagy and apicoplast formation. Autophagy 2013;9(10):1540-1552.

10. Bouchut A, Geiger JA, DeRocher AE, Parsons M. Vesicles bearing *Toxoplasma* apicoplast membrane proteins persist following loss of the relict plastid or Golgi body disruption. PLoS One 2014;9(11):e112096.

11. Heiny SR, Pautz S, Recker M, Przyborski JM. Protein Traffic to the *Plasmodium falciparum* Apicoplast: Evidence for a Sorting Branch Point at the Golgi. Traffic 2014;15(12):1290-1304.

12. Agrawal S, van Dooren GG, Beatty WL, Striepen B. Genetic evidence that an endosymbiont-derived endoplasmic reticulum-associated protein degradation (ERAD) system functions in import of apicoplast proteins. J Biol Chem 2009;284(48):33683-33691.

13. Hempel F, Felsner G, Maier UG. New mechanistic insights into pre-protein transport across the second outermost plastid membrane of diatoms. Mol Microbiol 2010;76(3):793-801.

14. Kalanon M, Tonkin CJ, McFadden GI. Characterization of two putative protein translocation components in the apicoplast of

Plasmodium falciparum. Eukaryot Cell 2009;8(8):1146-1154.

15. Spork S, Hiss JA, Mandel K, Sommer M, Kooij TW, Chu T, Schneider G, Maier UG, Przyborski JM. An unusual ERAD-like complex is targeted to the apicoplast of *Plasmodium falciparum*. Eukaryot Cell 2009;8(8):1134-1145.

16. Stork S, Moog D, Przyborski JM, Wilhelmi I, Zauner S, Maier UG. Distribution of the SELMA translocon in secondary plastids of red algal origin and predicted uncoupling of ubiquitin-dependent translocation from degradation. Eukaryot Cell 2012;11(12):1472-1481.

17. Glaser S, van Dooren GG, Agrawal S, Brooks CF, McFadden GI, Striepen B, Higgins MK. Tic22 is an essential chaperone required for protein import into the apicoplast. J Biol Chem 2012;287(47):39505-39512.

18. van Dooren GG, Tomova C, Agrawal S, Humbel BM, Striepen B. *Toxoplasma gondii* Tic20 is essential for apicoplast protein import. Proc Natl Acad Sci U S A 2008;105(36):13574-13579.

19. van Dooren GG, Su V, D'Ombrain MC, McFadden GI. Processing of an apicoplast leader sequence in *Plasmodium falciparum* and the identification of a putative leader cleavage enzyme. J Biol Chem 2002;277(26):23612-23619.

20. Gould SB, Sommer MS, Hadfi K, Zauner S, Kroth PG, Maier UG. Protein targeting into the complex plastid of cryptophytes. J Mol Evol 2006;62(6):674-681.

21. Gruber A, Vugrinec S, Hempel F, Gould SB, Maier UG, Kroth PG. Protein targeting into complex diatom plastids: functional characterisation of a specific targeting motif. Plant Mol Biol 2007;64(5):519-530.

22. Kilian O, Kroth PG. Identification and characterization of a new conserved motif within the presequence of proteins targeted into complex diatom plastids. Plant J 2005;41(2):175-183.

23. Patron NJ, Waller RF, Archibald JM, Keeling PJ. Complex protein targeting to dinoflagellate plastids. J Mol Biol 2005;348(4):1015-1024.

24. Steiner JM, Yusa F, Pompe JA, Loffelhardt W. Homologous protein import machineries in chloroplasts and cyanelles. Plant J 2005;44(4):646-652.

25. Wunder T, Martin R, Loffelhardt W, Schleiff E, Steiner JM. The invariant phenylalanine of precursor proteins discloses the importance of Omp85 for protein translocation into cyanelles. BMC Evol Biol 2007;7:236.

26. Deane JA, Fraunholz M, Su V, Maier UG, Martin W, Durnford DG, McFadden GI. Evidence for nucleomorph to host nucleus gene transfer: light-harvesting complex proteins from cryptomonads and chlorarachniophytes. Protist 2000;151(3):239-252.

27. Ralph SA, Foth BJ, Hall N, McFadden GI. Evolutionary pressures on apicoplast transit peptides. Mol Biol Evol 2004;21(12):2183-2194.

28. Harb OS, Chatterjee B, Fraunholz MJ, Crawford MJ, Nishi M, Roos DS. Multiple functionally redundant signals mediate targeting to the apicoplast in the apicomplexan parasite *Toxoplasma gondii*. Eukaryot Cell 2004;3(3):663-674.

29. Schleiff E, Becker T. Common ground for protein translocation: access control for mitochondria and chloroplasts. Nat Rev Mol Cell Biol 2011;12(1):48-59.

30. Simmerman RF, Dave AM, Bruce BD. Structure and function of POTRA domains of Omp85/TPS superfamily. Int Rev Cell Mol Biol 2014;308:1-34.

31. Gentle I, Gabriel K, Beech P, Waller R, Lithgow T. The Omp85 family of proteins is essential for outer membrane biogenesis in mitochondria and bacteria. J Cell Biol 2004;164(1):19-24.

32. Kozjak V, Wiedemann N, Milenkovic D, Lohaus C, Meyer HE, Guiard B, Meisinger C, Pfanner N. An essential role of Sam50 in the protein sorting and assembly machinery of the mitochondrial outer membrane. J Biol Chem 2003;278(49):48520-48523.

33. Eckart K, Eichacker L, Sohrt K, Schleiff E, Heins L, Soll J. A Toc75-like protein import channel is abundant in chloroplasts. EMBO Rep 2002;3(6):557-562.

34. Inoue K, Potter D. The chloroplastic protein translocation channel Toc75 and its paralog OEP80 represent two distinct protein families and are targeted to the chloroplastic outer envelope by different mechanisms. Plant J 2004;39(3):354-365.

35. Schleiff E, Soll J, Kuchler M, Kuhlbrandt W, Harrer R. Characterization of the translocon of the outer envelope of chloroplasts. J Cell Biol 2003;160(4):541-551.

36. Schnell DJ, Kessler F, Blobel G. Isolation of components of the chloroplast protein import machinery. Science 1994;266(5187):1007-1012.

37. Bullmann L, Haarmann R, Mirus O, Bredemeier R, Hempel F, Maier UG, Schleiff E. Filling the gap, evolutionarily conserved Omp85 in plastids of chromalveolates. J Biol Chem 2010;285(9):6848-6856.

38. Agrawal S, Striepen B. More membranes, more proteins: complex protein import mechanisms into secondary plastids. Protist 2010;161(5):672-687.

39. Hirakawa Y, Burki F, Keeling PJ. Genome-based reconstruction of the protein import machinery in the secondary plastid of a chlorarachniophyte alga. Eukaryot Cell 2012;11(3):324-333.

40. Sheiner L, Demerly JL, Poulsen N, Beatty WL, Lucas O, Behnke MS, White MW, Striepen B. A systematic screen to discover and analyze apicoplast proteins identifies a conserved and essential protein import factor. PLoS Pathog 2011;7(12):e1002392.

41. Brooks CF, Johnsen H, van Dooren GG, Muthalagi M, Lin SS, Bohne W, Fischer K,

Striepen B. The *Toxoplasma* apicoplast phosphate translocator links cytosolic and apicoplast metabolism and is essential for parasite survival. Cell Host Microbe 2010;7(1):62-73.

42. Francia ME, Jordan CN, Patel JD, Sheiner L, Demerly JL, Fellows JD, de Leon JC, Morrissette NS, Dubremetz JF, Striepen B. Cell division in Apicomplexan parasites is organized by a homolog of the striated rootlet fiber of algal flagella. PLoS Biol 2012;10(12):e1001444.

43. Waller RF, Keeling PJ, Donald RG, Striepen B, Handman E, Lang-Unnasch N, Cowman AF, Besra GS, Roos DS, McFadden GI. Nuclear-encoded proteins target to the plastid in *Toxoplasma gondii* and *Plasmodium falciparum*. Proc Natl Acad Sci U S A 1998;95(21):12352-12357.

44. Waller RF, Reed MB, Cowman AF, McFadden GI. Protein trafficking to the plastid of *Plasmodium falciparum* is via the secretory pathway. EMBO J 2000;19(8):1794-1802.

45. Nair SC, Brooks CF, Goodman CD, Sturm A, McFadden GI, Sundriyal S, Anglin JL, Song Y, Moreno SN, Striepen B. Apicoplast isoprenoid precursor synthesis and the molecular basis of fosmidomycin resistance in *Toxoplasma gondii*. J Exp Med 2011;208(7):1547-1559.

46. Gould SB, Sommer MS, Kroth PG, Gile GH, Keeling PJ, Maier UG. Nucleus-to-nucleus gene transfer and protein retargeting into a remnant cytoplasm of cryptophytes and diatoms. Mol Biol Evol 2006;23(12):2413-2422.

47. Kalanon M, McFadden GI. The chloroplast protein translocation complexes of *Chlamydomonas reinhardtii*: a bioinformatic comparison of Toc and Tic components in plants, green algae and red algae. Genetics 2008;179(1):95-112.

48. Huang W, Ling Q, Bedard J, Lilley K, Jarvis P. In vivo analyses of the roles of essential Omp85-related proteins in the chloroplast outer envelope membrane. Plant Physiol 2011;157(1):147-159.

49. Jarvis P, Chen LJ, Li H, Peto CA, Fankhauser C, Chory J. An Arabidopsis mutant defective in the plastid general protein import apparatus. Science 1998;282(5386):100-103.

50. Reumann S, Inoue K, Keegstra K. Evolution of the general protein import pathway of plastids (review). Mol Membr Biol 2005;22(1-2):73-86.

51. Tripp J, Hahn A, Koenig P, Flinner N, Bublak D, Brouwer EM, Ertel F, Mirus O, Sinning I, Tews I, Schleiff E. Structure and conservation of the periplasmic targeting factor Tic22 protein from plants and cyanobacteria. J Biol Chem 2012;287(29):24164-24173.

52. Bredemeier R, Schlegel T, Ertel F, Vojta A, Borissenko L, Bohnsack MT, Groll M, von Haeseler A, Schleiff E. Functional and phylogenetic properties of the pore-forming beta-barrel transporters of the Omp85 family. J Biol Chem 2007;282(3):1882-1890.

53. Eddy SR. Accelerated Profile HMM Searches. PLoS Comput Biol 2011;7(10):e1002195.

54. Finn RD, Bateman A, Clements J, Coggill P, Eberhardt RY, Eddy SR, Heger A, Hetherington K, Holm L, Mistry J, Sonnhammer EL, Tate J, Punta M. Pfam: the protein families database. Nucleic Acids Res 2014;42(Database issue):D222-230.

55. Flinner N, Ellenrieder L, Stiller SB, Becker T, Schleiff E, Mirus O. Mdm10 is an ancient eukaryotic porin co-occurring with the ERMES complex. Biochim Biophys Acta 2013;1833(12):3314-3325.

56. Stamatakis A. RAxML version 8: a tool for phylogenetic analysis and post-analysis of large phylogenies. Bioinformatics 2014;30(9):1312-1313.

57. Whelan S, Goldman N. A general empirical model of protein evolution derived from multiple protein families using a maximum-likelihood approach. Mol Biol Evol 2001;18(5):691-699.

58. Reiff SB, Vaishnava S, Striepen B. The HU protein is important for apicoplast genome maintenance and inheritance in *Toxoplasma gondii*. Eukaryot Cell 2012;11(7):905-915.

59. Schindelin J, Arganda-Carreras I, Frise E, Kaynig V, Longair M, Pietzsch T, Preibisch S, Rueden C, Saalfeld S, Schmid B, Tinevez JY, White DJ, Hartenstein V, Eliceiri K, Tomancak P*, et al.* Fiji: an open-source platform for biological-image analysis. Nat Methods 2012;9(7):676-682.

60. Agrawal S, Chung DW, Ponts N, van Dooren GG, Prudhomme J, Brooks CF, Rodrigues EM, Tan JC, Ferdig MT, Striepen B, Le Roch KG. An apicoplast localized ubiquitylation system is required for the import of nuclear-encoded plastid proteins. PLoS Pathog 2013;9(6):e1003426.

61. Soding J, Biegert A, Lupas AN. The HHpred interactive server for protein homology detection and structure prediction. Nucleic Acids Res 2005;33(Web Server issue):W244-248.

Figure legends

Figure 1 *Machinery and signals involved in the translocation of precursor protein through the apicoplast membranes*. (A) Schematic representation of the translocation machinery responsible for protein import through the four membranes of the apicoplast. Endomembrane system shown in grey, former red algal cytosol in blue and former primary plastid in pink. According to the current model of transport apicoplast precursor proteins are first co-translationally transported into the ER via the SEC61 complex courtesy of their signal peptide (SP). In the ER lumen, the SP is cleaved by a signal peptide peptidase (SiPP). The now exposed transit peptide (TP) signals for transport from the ER to the apicoplast. Next, the translocation through ERAD/SELMA is likely accompanied by transient ubiquitination (60). The protein then moves through the TOC and TIC complexes and its TP is cleaved in the stroma. Compartmental markers used in this study are depicted at the upper right corner of their corresponding compartment. (B) Abundance of residues at position +1 of 29 proteins experimentally confirmed to localize to the apicoplast stroma (i) or peripheral compartments (ii) based on SP cleavage prediction by SignalP (detailed analysis is provided in TableS1). (C) High-resolution microscopy analysis of the localization of transiently expressed ACP-YFP with the wild type phenylalanine and tyrosine at the two predicted potential position +1 (i) with tyrosine to alanine mutation (ii) and with phenylalanine to alanine mutation (iii). Full SP sequence is shown with arrows showing both potential +1 residues in the wild type, or the position of mutation to alanine in the mutants. The upper panels show co-staining with the stromal marker CPN60 and the lower panels show co-staining with the PPC marker ATrx2 (40).

Figure 2 *Phylogenetic classification of Omp85-like proteins in* T. gondii *and* P. falciparum.
A majority rule consensus tree of selected Sam50 and Toc75 homologs was constructed with RAxML from 1,000 bootstrap trees. The corresponding maximum likelihood (ML) tree is given in Figure S1A. The proteins are referenced by their ID (GenBank, or EupathDB); species abbreviations are as follows: Anig (*Aspergillus niger* ATCC 1015), Atha (*Arabidopsis thaliana*), Bden (*Batrachochytrium dendrobatidis* JAM81), Cmer (*Cyanidioschyzon merolae* strain 10D), Cowc (*Capsaspora owczarzaki* ATCC 30864), Crei (*Chlamydomonas reinhardtii*), Dmel (*Drosophila melanogaster*), Esil (*Ectocarpus siliculosus*), Gsul (*Galdieria sulphuraria*), Hvul (*Hydra vulgaris*), Mocc (*Metaseiulus occidentalis*), Otau (*Ostreococcus tauri*), Pfal (*Plasmodium falciparum* 3D7), Pmar (*Perkinsus marinus* ATCC 50983), Ppat (*Physcomitrella patens*), Ptri (*Phaeodactylum tricornutum* CCAP 1055/1), Rirr (*Rhizophagus irregularis* DAOM 197198w), Rnor (*Rattus norvegicus*), Scer (*Saccharomyces cerevisiae* S288c), Skow (*Saccoglossus kowalevskii*), Spur (*Strongylocentrotus purpuratus*), Tgon (*Toxoplasma gondii* ME49), Tura (*Triticum urartu*), Vcar (*Volvox carteri* f. nagariensis). The full alignments used for this analysis are provided in Figure S1.

Figure 3. *Localization of the omp85-like proteins supports their affiliation as Toc75 and Sam50 in Apicomplexa.* (A) Fluorescence microscopy analysis of *P. falciparum* parasites expressing ectopic GFP fusions of the 78 (upper panel) and 95 (middle panels) N-terminal amino acids of PfToc75, and of *T. gondii* parasites expressing ectopic HA-tagged full-length TgToc75 (lower panel). Co-staining is done with ACP and FNR-RFP for *P. falciparum* and *T. gondii* respectively. (B) High-resolution microscopy of transiently expressed full-length Ty tagged TgToc75 and its localization with respect to the stromal marker CPN60. (C) *P. falciparum* parasite expressing ectopic GFP fusion of the 60 N-terminal amino acids of PfSam50 (green channel) co-stained with mito-tracker (red channel) (upper panel); *T. gondii* parasites expressing ectopic Ty-tagged TgSam50 (green channel) co-stained with the mitochondrial marker HSP60-RFP (red channel) (lower panel). (D) *T. gondii* parasites co-expressing ectopic HA-tagged TgToc75 (red channel) and Ty-tagged TgSam50 (green channel).

Figure 4. *TgToc75 is essential for parasite growth and apicoplast maintenance*. (A) Schematic representation of the manipulation of the *TgToc75* locus to replace the native promoter with the tetracycline inducible promoter. Black boxes – exons; asterisk – stop codon; empty boxes – minigenes; solid lines – TgToc75 locus non-coding sequences; dashed line – genomic sequence; grey thick line – backbone of cosmid or of modification cassette. (B) Plaque assays performed with the *TATiΔKu80iToc75pr* parasite line in the absence (-) or presence (+) of ATc. (C) qRT-PCR analysis with RNA extracts from *TATiΔKu80iToc75pr* grown in the absence of ATc (-ATc) or upon down regulation of TgToc75 for 24 (+24h) and 72 (+72h) hours. TgToc75 mRNA levels decline swiftly upon ATc treatment. Y-axis shows the percentage of wild type copy numbers. (D) *TATiΔKu80iToc75pr* parasites were grown in ATc as indicated and plastids were counted based on immunofluorescence signal obtained via staining with anti-CPN60 antibody in 100 four-parasites vacuoles for each sample. Y-axis shows percentage of 4-parasites-vacuoles. (E) Apicoplast loss was also evaluated using qPCR comparing nuclear genome and apicoplast genome copy numbers. The data was normalized such that copy number from each genome from no ATc treatment is 1. In support of apicoplast loss the proportion of apicoplast copy number after TgToc75 down-regulation for 72 hours is on average 0.17 while genomic copy number average proportion is 0.78.

Figure 5. *TgToc75 down regulation results in deficient import of stromal but not PPC or outer membrane compartment apicoplast proteins*. We performed western blot analysis to follow the

maturation of apicoplast proteins under the down regulation of apicoplast import components. The steady state expression of endogenously YFP-tagged ACP (40) (A) and of endogenously HA-tagged TGME49_001270 (B) was monitored at each time point of *TgToc75* down regulation showing maturation defect in ACP but not TGME49_001270 at 72 hours. Western blot analysis following the maturation of the same makers (YFP-tagged ACP (C) and endogenously HA-tagged TGME49_001270 (D)), but this time under down regulation of the PPC import component *TgPPP1,* shows maturation defect for both at 48 hours. We then performed western blot analysis following the maturation of the stromal protein LytB-Ty (E) and the periplastid protein PPP1 (F). In this experiment LytB or PPP1 are transiently expressed for 24h at each time point of *TgToc75* down regulation. This analysis reveals a block in LytB maturation that is first detected at 24 hours and complete by 48 hours. In contrast, maturation defect of PPP1 is only observed at 72 hours. Loading control performed with anti-alpha-tubulin antibody is shown for each blot.

Figure S1 – *Phylogenetic classification of Omp85-like proteins in* T. gondii *and* P. falciparum.
Maximum likelihood (ML) phylogenies were reconstructed with RAxML. Branch support values were determined from 1,000 bootstrap trees. Sam50 and Toc75 clades are marked by dark and light gray areas, respectively. The sequence labels are colored according to their taxonomy (color code given in Figure 2). (A) The ML tree was reconstructed from the same set of sequences as used for the majority rule consensus tree in Figure 2. (B) This ML tree was reconstructed with the same sequences as (A) while including PfToc75. (C) From the multiple sequence consensus alignment as used for the trees above the N-terminal part containing the POTRA domains was excised and a ML tree reconstructed. (D) The full alignments used for these phylogenies (also available in other formats upon request).

Figure S2 – *The N-terminal domain of TgToc75 is sufficient for apicoplast localization.* Fluorescence microscopy analysis of parasites expressing ectopic Ty-tagged fusions of the 78 (upper panel) and 95 (lower panels) N-terminal amino acids of TgToc75. Note that the Ty tags are directly fused to the 78 or 95 amino acids with no spacer sequences.

Figure S3 – *TgToc75 is essential for parasite growth and apicoplast biogenesis*. (A) Schematic representation of the manipulation of the *TgToc75* locus to insert the tetracycline inducible promoter between the native promoter and the ORF. (B) Plaque assays performed with the *TATiΔKu80iToc75pi* parasite line in the absence (-) or presence (+) of ATc which correspond to TgToc75 constitutive levels or down-regulation respectively. (C) Fluorescence microscopy of *TATiΔKu80iToc75pi* grown in absence of ATc (-ATc) or upon down-regulation of TgToc75 for 72 hours (+ATc 72h) stained with the apicoplast marker CPN60 (12) showing loss of apicoplast in most parasites at this time point. (D) Pulse-chase (*P/C*) analysis of protein synthesis and post-translational lipoylation of apicoplast (PDH-E2) and mitochondrial (mito-E2) proteins. Parasites were metabolically labeled as detailed in (12, 18, 40) and lipoylated proteins were isolated by immunoprecipitation using a specific antibody. Lipoylation of PDH-E2 is lost upon ATc treatment. Bands labeled with an asterisk likely represent lipoylated host cell proteins

Table 1 – GeneIDs and summary of targeting prediction for apicomplexan Omp85-like protein encoding genes

Table S1 – Prediction of signal peptide cleavage and amino acid at position +1 of putative transit peptide for 47 experimentally confirmed apicoplast proteins.

Table S2 – Primers used in this study

List of supplemental materials:

Material included	Main text associate	Significance
Text + Figure S1	Result paragraph 1	Provides detailed explanation on sequence identification experimental confirmation and phylogenetic analysis allowing expert reader to critically follow the process. Provides the alignments used for the phylogenetic analyses.
Table S1	Figure 1B	Raw data of results summarized in the graphs. Reader can extract more information: the specific gene IDs used and the scores for each data point.
Table S2	Materials and methods	List of all primers used for genetic manipulations described in the text. Technical details for reader who wishes to perform similar manipulations.
Figure S2	Figure 3	Allows the reader to compare the localization pattern observed with the N-terminal fusion to the full-length that appears in the main text. In some organisms N-terminal fusion is more common. Showing that both generate the same localization validates this approach.
Figure S3	Figure 4	Provide evidence to an important difference between two approaches of genetic manipulation that are commonly used in *T. gondii*. Provides an additional independent assessment of Toc75's role in apicoplast biogenesis.

Supplementary text

Sequence analysis of omp85-like proteins in Apicomplexa genomes

We used jackhmmer to mine the NCBI non-redundant database with *Arabidopsis thaliana* Toc75-III as query sequence. This search revealed two Omp85-like protein coding genes in *T. gondii* ME49 (TGME49_205570, TGME49_272390) and in several *Plasmodium* spp (Table 1). Subsequent Omp85-related pHMM searches in the PFAM database, and a BLAST search using the above detected *Toxoplasma* and *Plasmodium* Omp85 proteins unraveled two Omp85-like proteins also in *P. falciparum* 3D7 (PF3D7_0608310 and PF3D7_1234600). Reciprocal BLASTs against the apicomplexan databases in EupathDB (http://eupathdb.org/eupathdb/) identified further homologs of both proteins encoded by several species (Table 1).

The predicted gene models for TgToc75 and PfToc75 as found on EupathDB were changed since we first identified these genes: TgToc75 older version, TGME49_072390 includes an extreme C-terminal domain, which is part of the predicted β-barrel. This C-terminal domain is missing in the new version (TGME49_272390). Our RT-PCR and localization of full-length protein supports the old gene models. Similarly, PfToc75's previous model (PFF0410w) predicts one continuous gene, which is now predicted to be two separate genes (PF3D7_0608300/0608310). Our RT-PCR confirms the old model. Prediction of organelle targeting signals as shown in table 1 used the older experimentally confirmed gene models. User comments were added to the respective gene pages in ToxoDB and PlasmoDB.

To determine the affiliations of the four identified Omp85-like sequences from *Plasmodium falciparum* and *Toxoplasma gondii*, we selected a subset of species across the eukaryotic tree of life and generated a sequence alignment as described in (55). A majority rule consensus tree was then constructed from 1,000 bootstrap trees based on this alignment (Figure 2). A maximum likelihood (ML) phylogeny was reconstructed from the same dataset with RAxML. Branch support values were determined from 1,000 bootstrap trees (Figure S1A). We then added the second *Plasmodium falciparum* Omp85 sequence that was not originally identified via the jackhmmer search (PF3D7_1234600) to the dataset and reconstructed another ML tree (Figure S1B). However, the classification of this sequence is ambiguous. We set out to clarify its affiliation by constructing a phylogenetic tree of the excised POTRA region, which is more conserved than the β-barrel region and thus more suitable for the tree reconstruction. This tree shows that PF3D7_1234600 is located within the sub-tree containing the other Toc75 homologs from Chromalveolates (Figure 2B). Furthermore, the bootstrap between the Sam50 and Toc75 clades is reliable with a value of 88. In our alignment we could identify two POTRA domains in PfToc75 (residues 118-192, 193-454) and TgToc75 (189-336, 337-451), which are in agreement with fold recognition results except that the HHpred webserver (61) does not detect the 1st β-strand of PfToc75's 2nd POTRA domain (399-454). In agreement with the assignment based on the phylogenetic trees PfToc75 possesses a predicted apicoplast-targeting signal and for PfSam50 a mitochondrial targeting sequence was predicted (Table 1).

Supplementary references

1. Flinner N, Ellenrieder L, Stiller SB, Becker T, Schleiff E, Mirus O. Mdm10 is an ancient eukaryotic porin co-occurring with the ERMES complex. Biochim Biophys Acta 2013;1833(12):3314-3325.
2. Soding J, Biegert A, Lupas AN. The HHpred interactive server for protein homology detection and structure prediction. Nucleic Acids Res 2005;33(Web Server issue):W244-248.

Figure 1

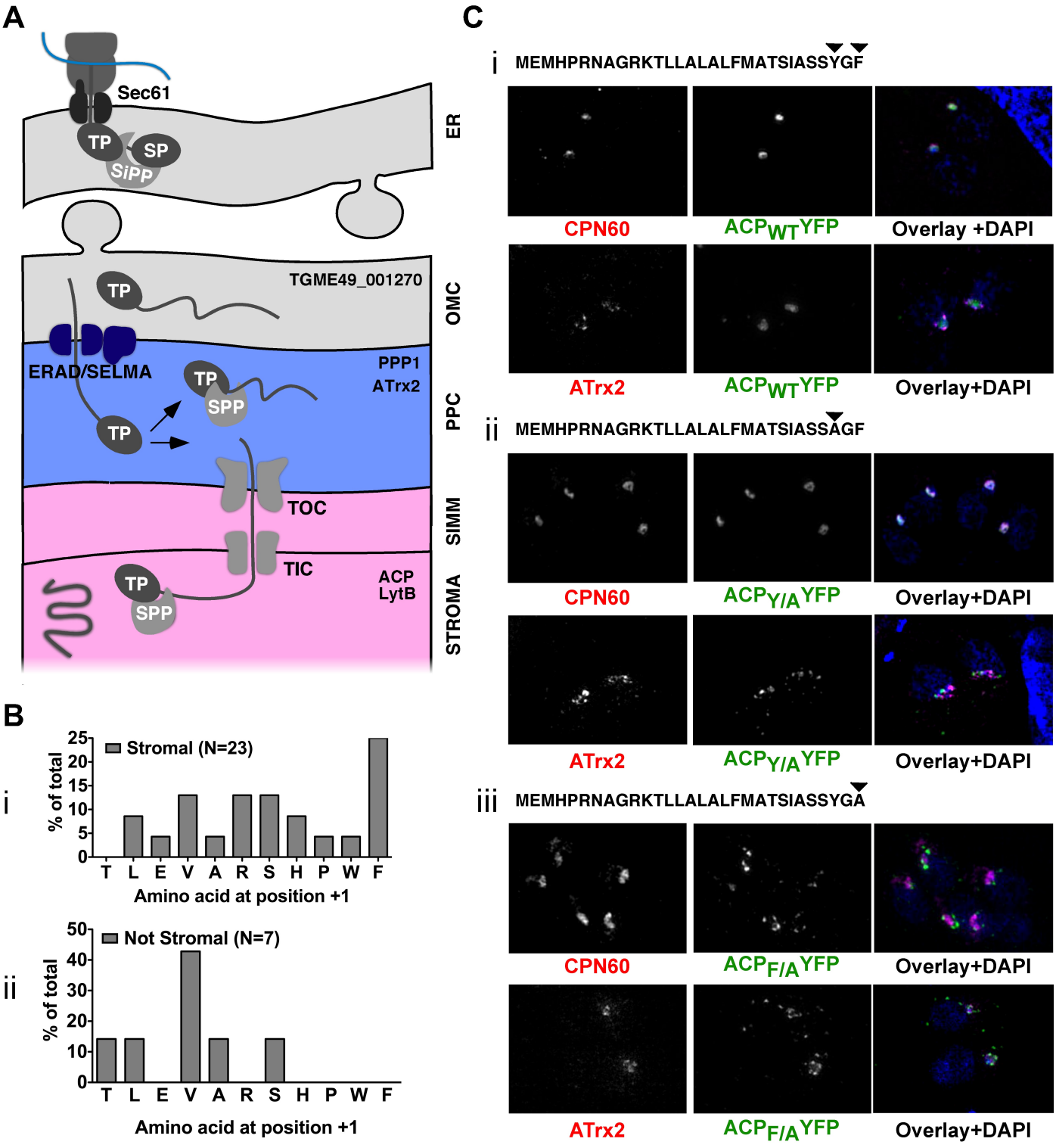
A
Sec61
TP
SP
SiPP
ER
TGME49_001270
TP
OMC
ERAD/SELMA
PPP1
ATrx2
TP
SPP
TP
PPC
TOC
SIMM
TIC
ACP
LytB
TP
SPP
STROMA
B
i
Stromal (N=23)
% of total
25
20
15
10
5
0
T L E V A R S H P W F
Amino acid at position +1
ii
Not Stromal (N=7)
% of total
50
40
30
20
10
0
T L E V A R S H P W F
Amino acid at position +1
C
i MEMHPRNAGRKTLLALALFMATSIASSYGF
CPN60
ACPWTYFP
Overlay +DAPI
ATrx2
ACPWTYFP
Overlay+DAPI
ii MEMHPRNAGRKTLLALALFMATSIASSAGF
CPN60
ACPY/AYFP
Overlay+DAPI
ATrx2
ACPY/AYFP
Overlay+DAPI
iii MEMHPRNAGRKTLLALALFMATSIASSYGA
CPN60
ACPF/AYFP
Overlay+DAPI
ATrx2
ACPF/AYFP
Overlay+DAPI

Figure 2

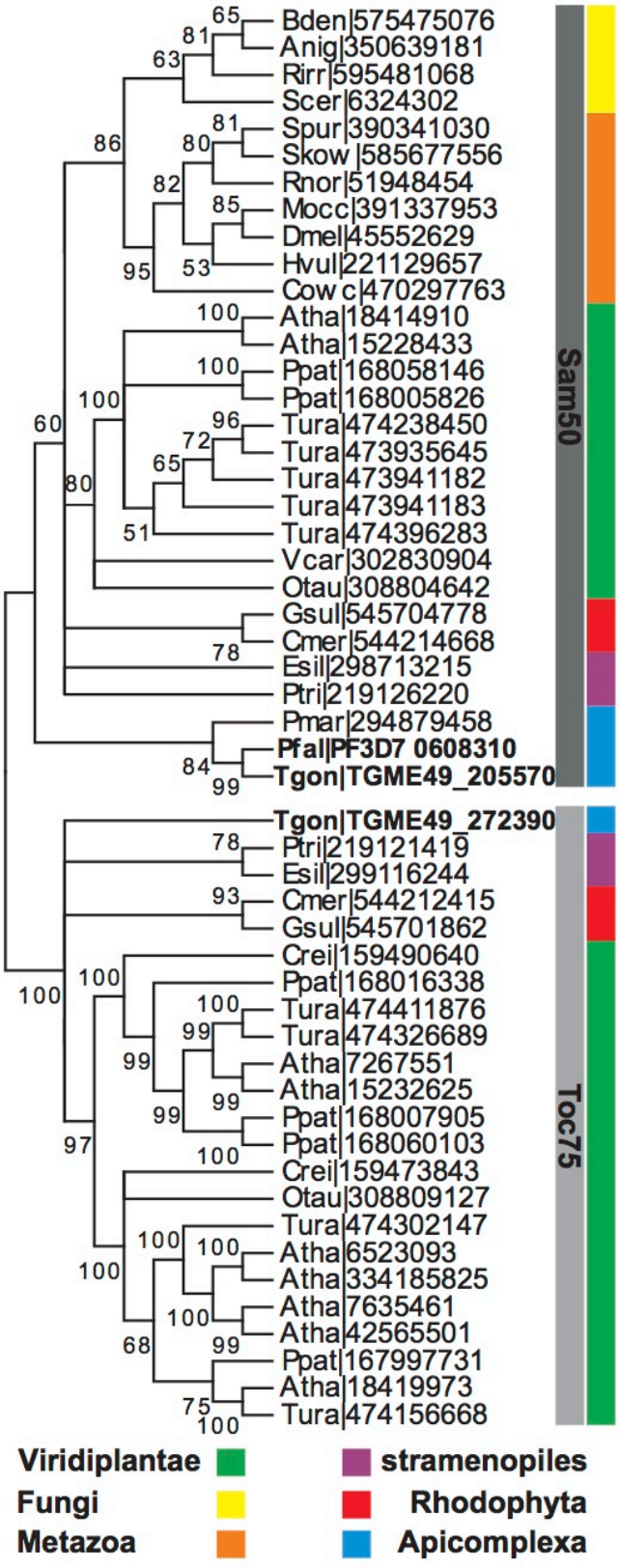
Bden|575475076
Anig|350639181
Rirr|595481068
Scer|6324302
Spur|390341030
Skow|585677556
Rnor|51948454
Mocc|391337953
Dmel|45552629
Hvul|221129657
Cowc|470297763
Atha|18414910
Atha|15228433
Ppat|168058146
Ppat|168005826
Tura|474238450
Tura|473935645
Tura|473941182
Tura|473941183
Tura|474396283
Vcar|302830904
Otau|308804642
Gsul|545704778
Cmer|544214668
Esil|298713215
Ptri|219126220
Pmar|294879458
Pfal|PF3D7 0608310
Tgon|TGME49_205570
Tgon|TGME49_272390
Ptri|219121419
Esil|299116244
Cmer|544212415
Gsul|545701862
Crei|159490640
Ppat|168016338
Tura|474411876
Tura|474326689
Atha|7267551
Atha|15232625
Ppat|168007905
Ppat|168060103
Crei|159473843
Otau|308809127
Tura|474302147
Atha|6523093
Atha|334185825
Atha|7635461
Atha|42565501
Ppat|167997731
Atha|18419973
Tura|474156668
Sam50
Toc75
Viridiplantae
Fungi
Metazoa
stramenopiles
Rhodophyta
Apicomplexa

Figure 3

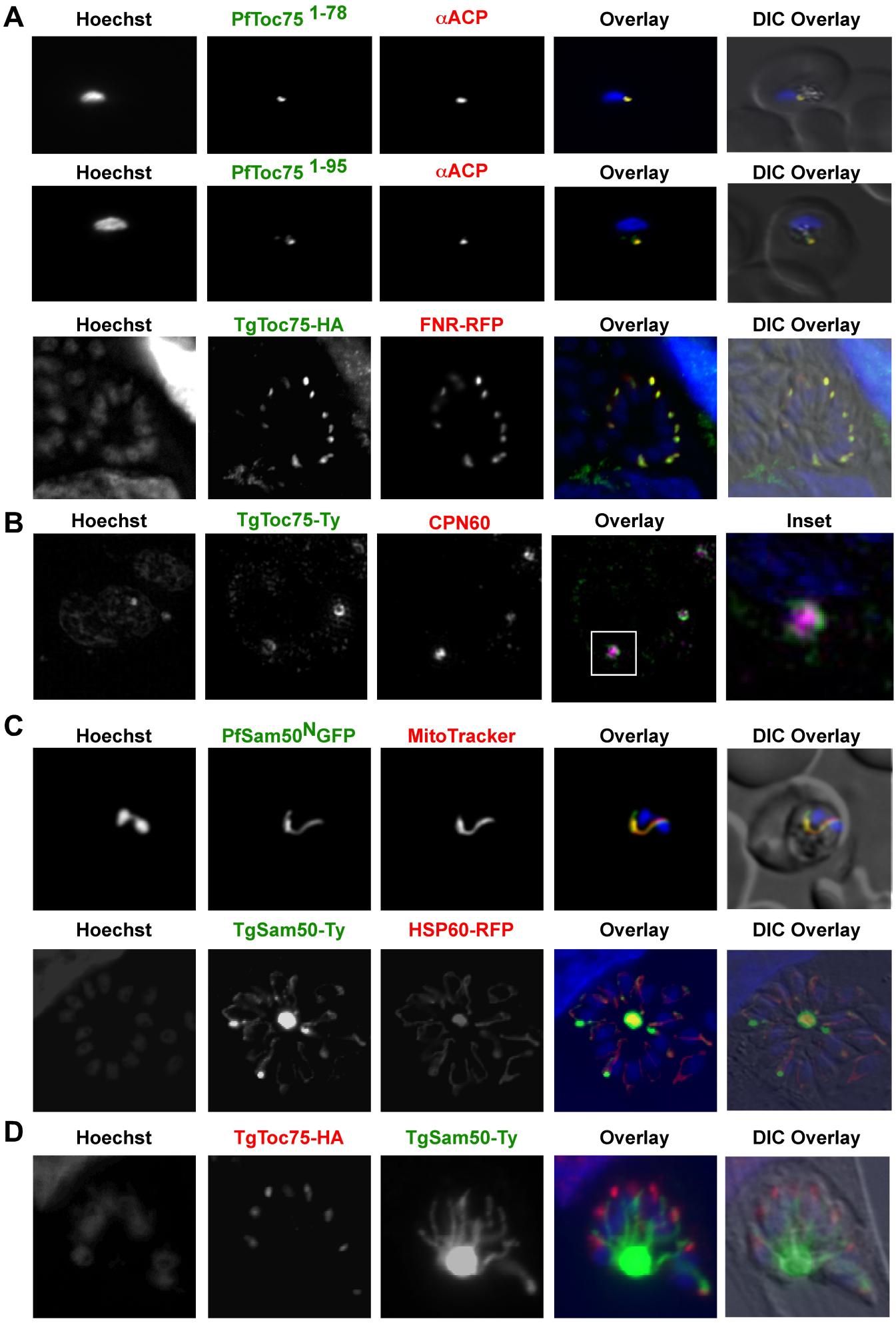
A
Hoechst
PfToc75 1-78
αACP
Overlay
DIC Overlay
Hoechst
PfToc75 1-95
αACP
Overlay
DIC Overlay
Hoechst
TgToc75-HA
FNR-RFP
Overlay
DIC Overlay
B
Hoechst
TgToc75-Ty
CPN60
Overlay
Inset
C
Hoechst
PfSam50NGFP
MitoTracker
Overlay
DIC Overlay
Hoechst
TgSam50-Ty
HSP60-RFP
Overlay
DIC Overlay
D
Hoechst
TgToc75-HA
TgSam50-Ty
Overlay
DIC Overlay

Figure 4

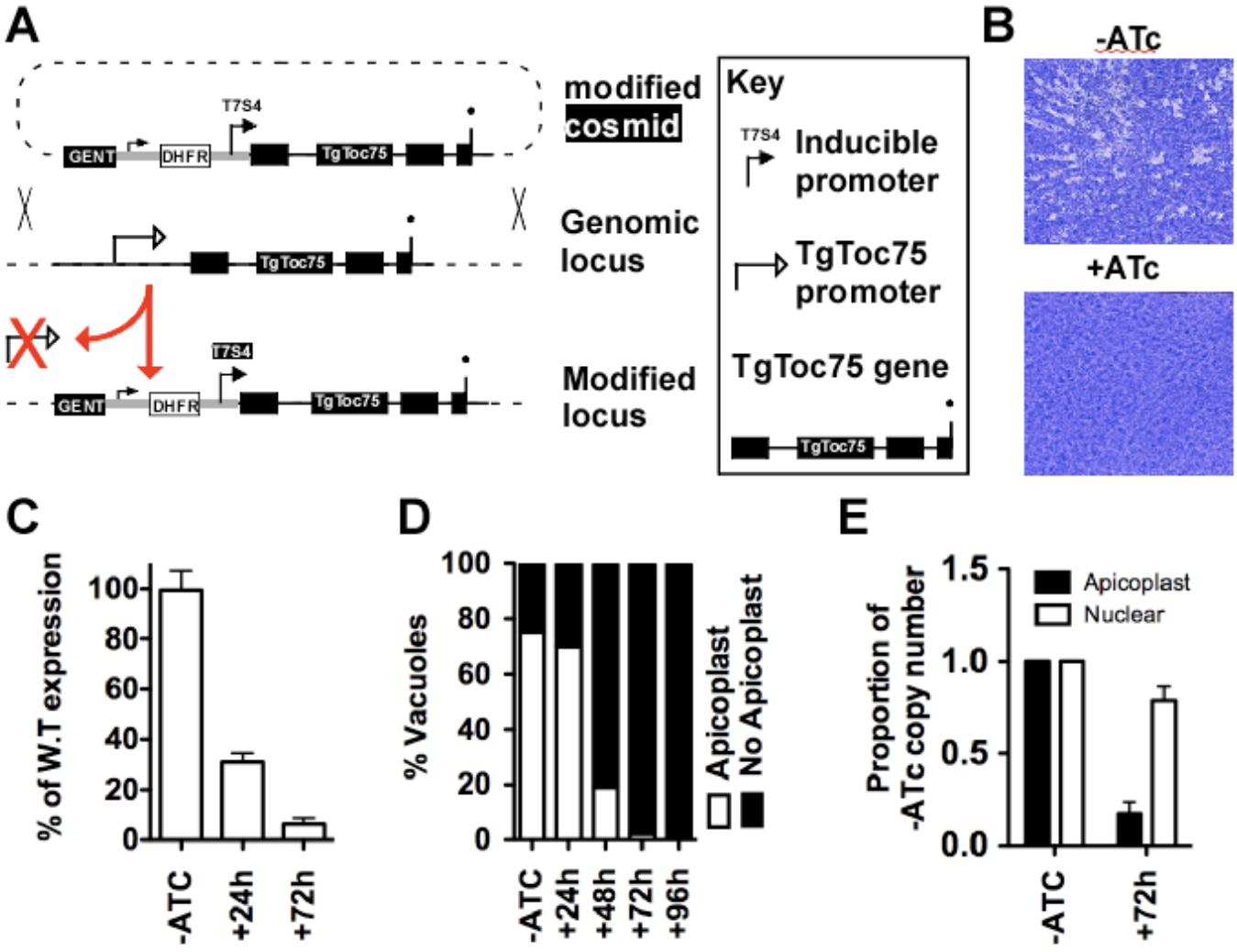
A
modified cosmid
Genomic locus
Modified locus
T7S4
GENT
DHFR
TgToc75
Key
Inducible promoter
TgToc75 promoter
TgToc75 gene
B
-ATc
+ATc
C
% of W.T expression
100
80
60
40
20
0
-ATC
+24h
+72h
D
% Vacuoles
Apicoplast
No Apicoplast
-ATC
+24h
+48h
+72h
+96h
E
Proportion of -ATc copy number
1.5
1.0
0.5
0.0
Apicoplast
Nuclear
-ATC
+72h

Figure 5

Steady state protein level

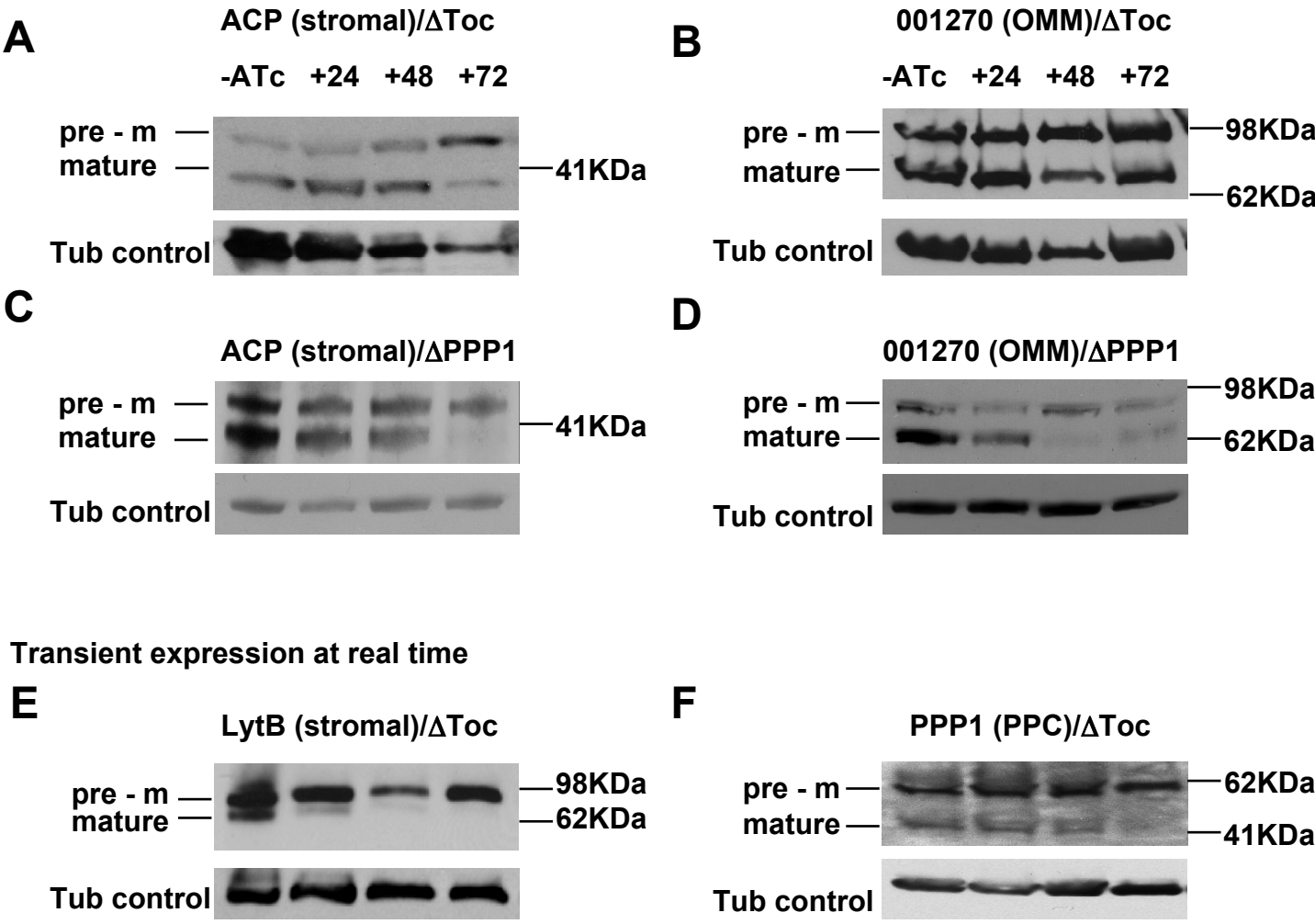

Transient expression at real time

Figure S1A

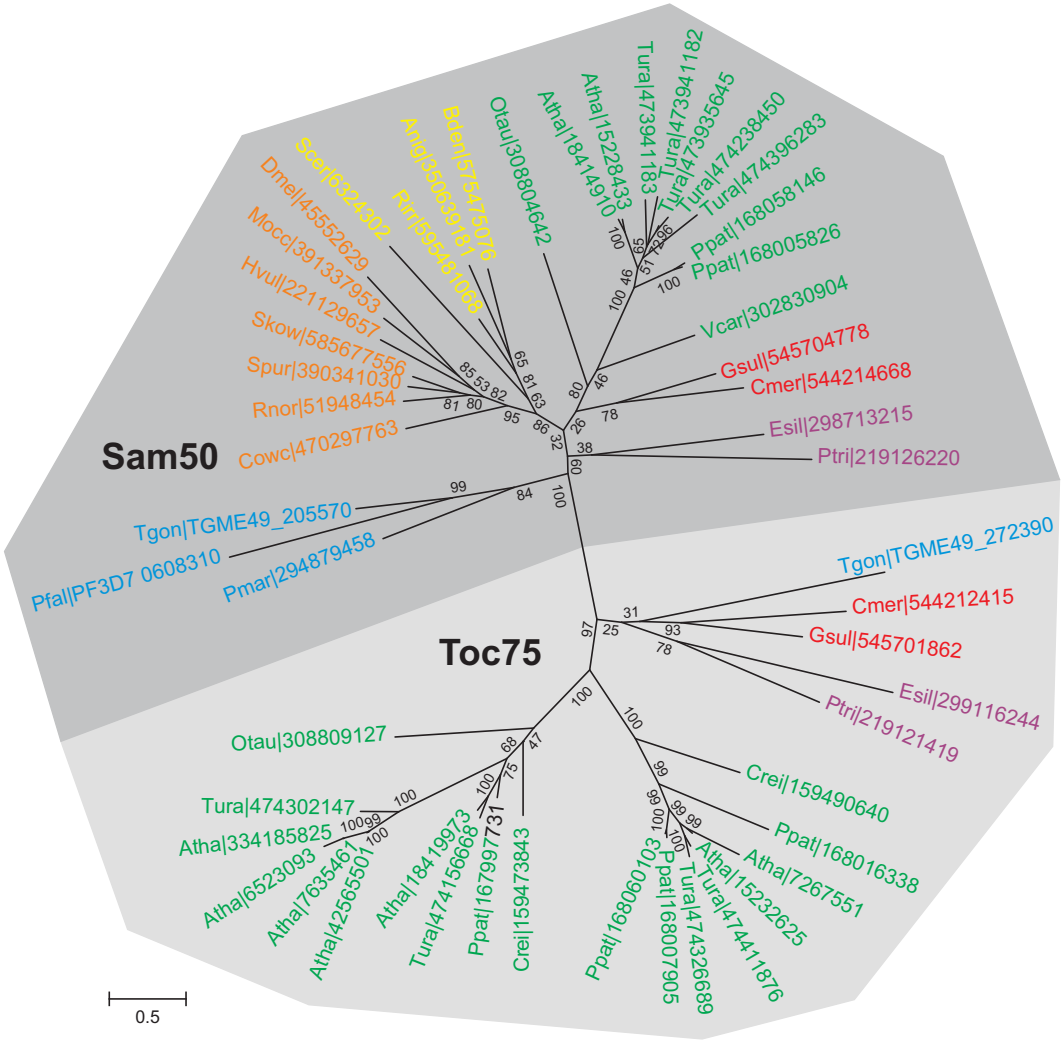
Sam50
Toc75
Tura|473941182
Tura|473941183
Tura|473935645
Tura|474238450
Tura|474396283
Ppat|168058146
Ppat|168005826
Vcar|302830904
Gsul|545704778
Cmer|544214668
Esil|298713215
Ptri|219126220
Atha|15228433
Atha|18414910
Otau|30880642
Bden|57547507
Scal|8324302
Dmel|45552629
Mocc|391337953
Hvul|221129657
Skow|585677556
Spur|390341030
Rnor|51948454
Cowc|470297763
Tgon|TGME49_205570
Pfal|PF3D7 0608310
Pmar|294879458
Tgon|TGME49_272390
Cmer|544212415
Gsul|545701862
Esil|299116244
Ptri|219121419
Otau|308809127
Tura|474302147
Atha|334185825
Atha|6523093
Atha|7635461
Atha|42565501
Atha|18419973
Tura|474156668
Ppat|167997731
Crei|159473843
Crei|159490640
Ppat|168016338
Atha|7267551
Atha|15232625
Tura|474411876
Tura|474326689
Ppat|168007905
Ppat|168060103
0.5

Figure S1B

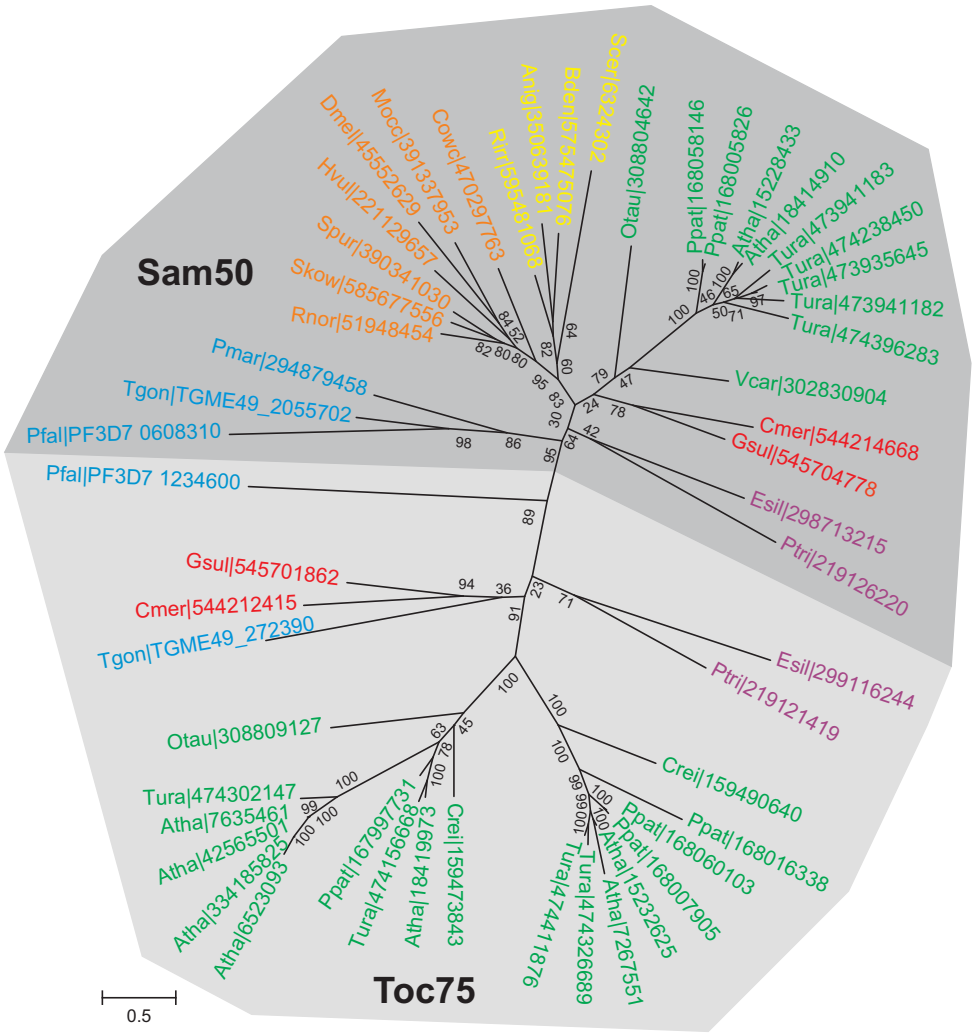
Sam50
Toc75
Dmel|45552629
Mocc|391337953
Cowc|470297763
Rbri|595481053
Anig|350639181
Eden|575475076
Scar|6321302
Otau|308804642
Ppat|168058146
Ppat|168005826
Atha|15228433
Atha|18414910
Tura|473941183
Tura|474238450
Tura|473935645
Tura|473941182
Tura|474396283
Hvul|221129657
Spur|390341030
Skow|585677556
Rnor|51948454
Pmar|294879458
Tgon|TGME49_2055702
Pfal|PF3D7 0608310
Pfal|PF3D7 1234600
Vcar|302830904
Cmer|544214668
Gsul|545704778
Esil|298713215
Ptri|219126220
Gsul|545701862
Cmer|544212415
Tgon|TGME49_272390
Esil|299116244
Ptri|219121419
Otau|308809127
Crei|159490640
Ppat|168016338
Ppat|168060103
Ppat|168007905
Atha|1523625
Atha|7267551
Tura|474326689
Tura|474411876
Crei|159473843
Atha|18419973
Ppat|167997731
Tura|474156668
Atha|6523093
Atha|33418582
Atha|42565501
Atha|7635461
Tura|474302147
0.5

Figure S1C

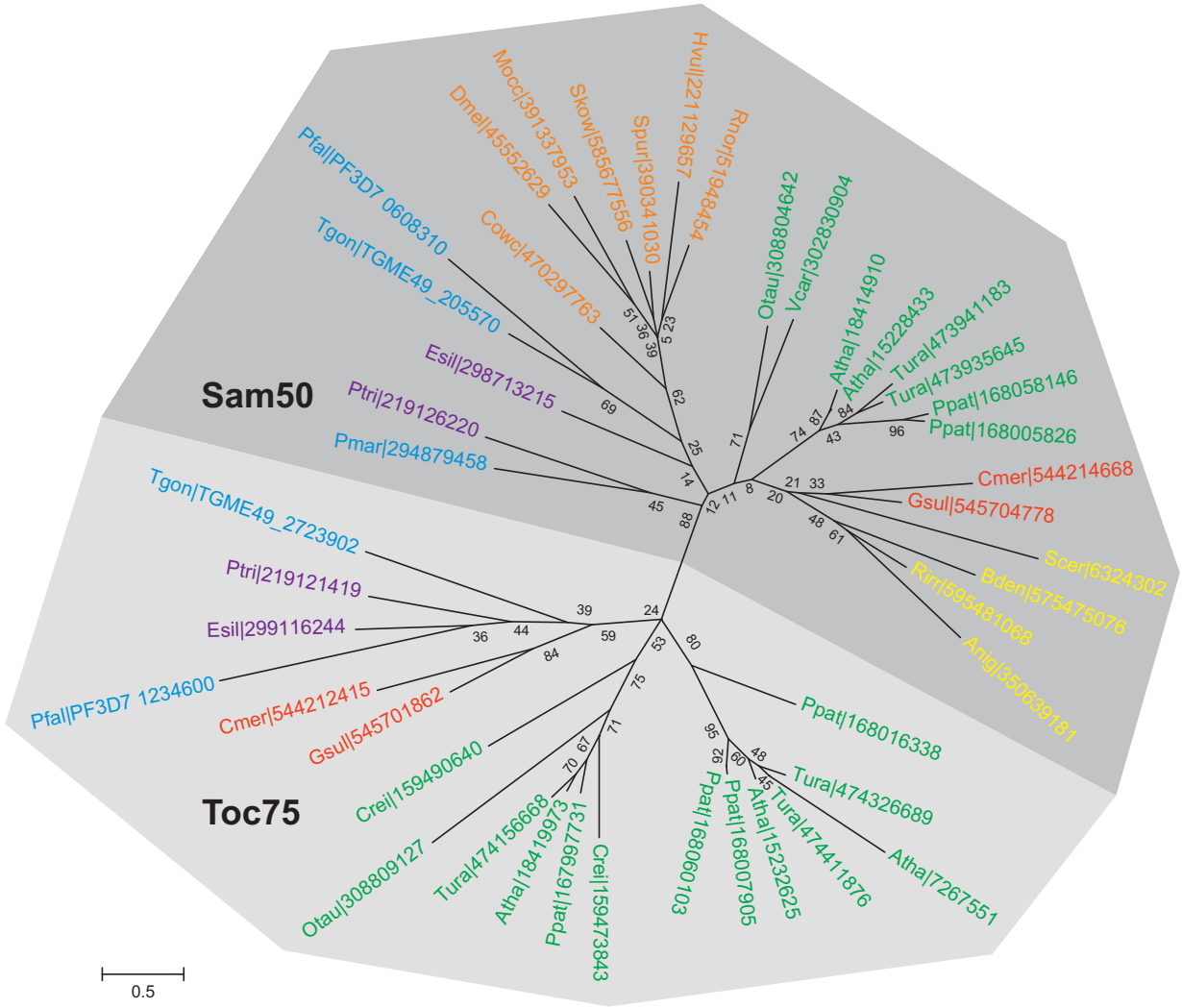
Sam50
Toc75
Hvul|221129657
Rnor|51948454
Spur|39034030
Skow|585677556
Mocc|391337953
Dmel|45552629
Cowc|470297763
Pfal|PF3D7 0608310
Tgon|TGME49_205570
Esil|298713215
Ptri|219126220
Pmar|294879458
Otau|308804942
Vcar|302830904
Atha|18414910
Atha|15228433
Tura|473941183
Tura|473935645
Ppat|168058146
Ppat|168005826
Cmer|544214668
Gsul|545704778
Scer|6324302
Bden|575475076
Rtri|595481088
Acry|340538181
Tgon|TGME49_2723902
Ptri|219121419
Esil|299116244
Pfal|PF3D7 1234600
Cmer|544212415
Gsul|545701862
Crei|159490640
Otau|308809127
Tura|474156668
Atha|18419973
Ppat|167997731
Crei|159473843
Ppat|168060103
Ppat|168007905
Atha|15232625
Tura|474411876
Atha|7267551
Ppat|168016338
Tura|474326689
0.5

Figure S2

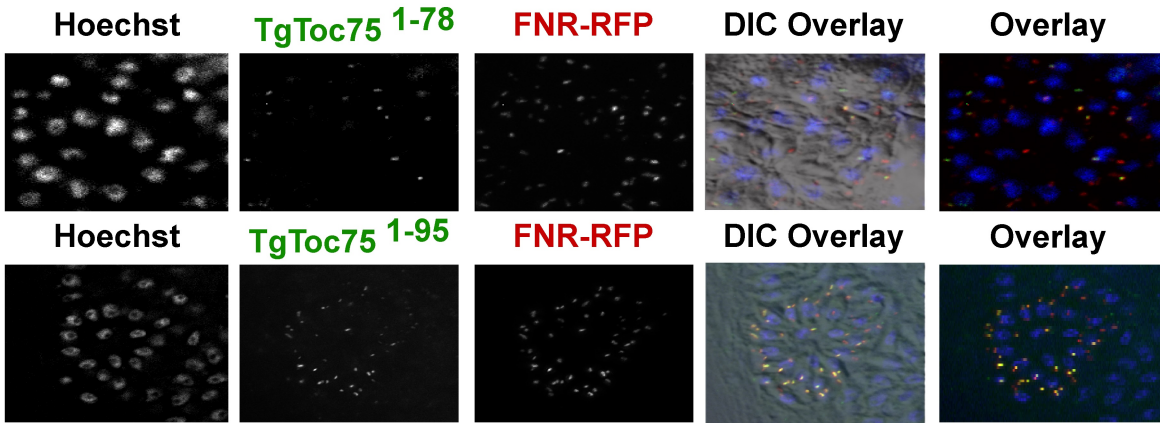
Hoechst
TgToc75 1-78
FNR-RFP
DIC Overlay
Overlay
Hoechst
TgToc75 1-95
FNR-RFP
DIC Overlay
Overlay

Figure S3

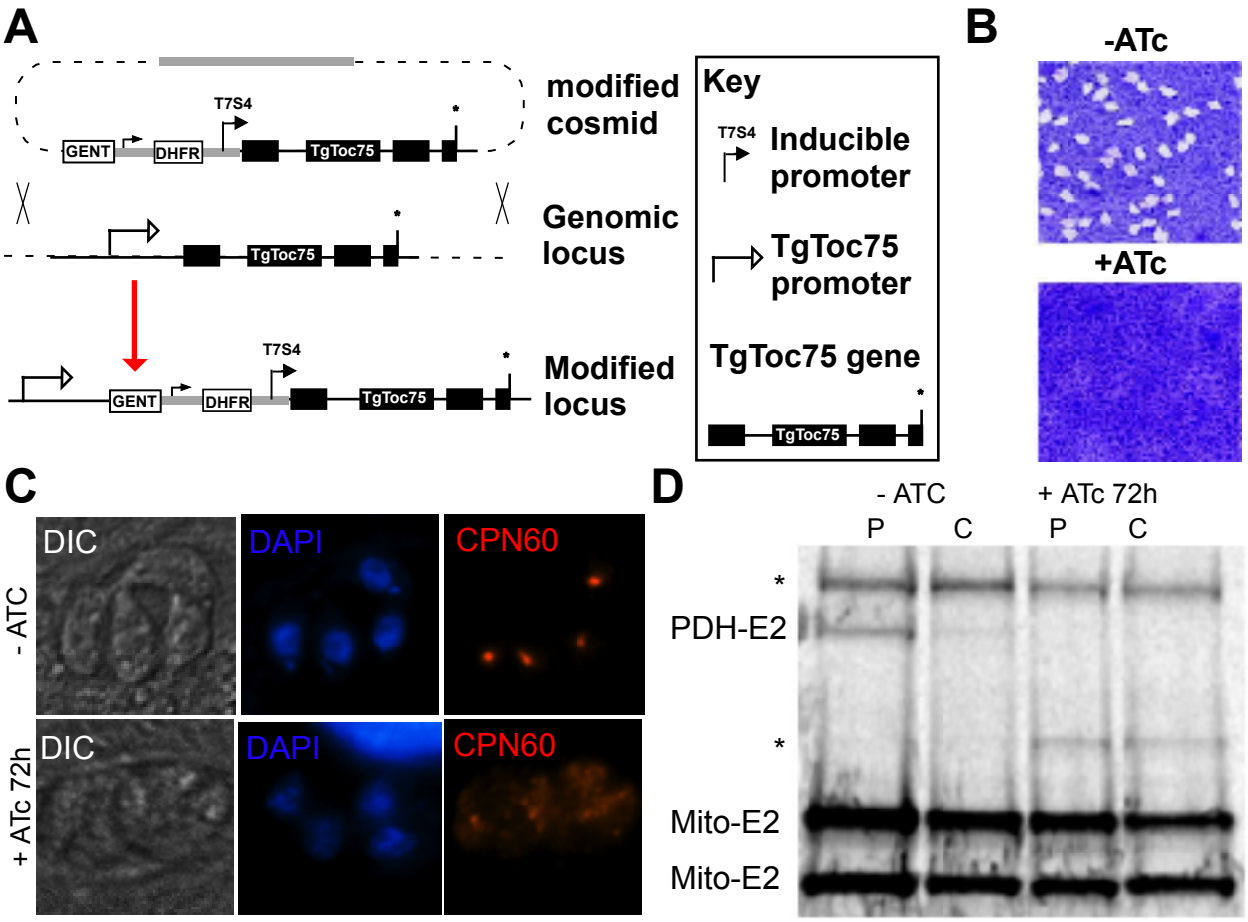
A
T7S4
GENT
DHFR
TgToc75
modified cosmid
Genomic locus
Modified locus
Key
Inducible promoter
TgToc75 promoter
TgToc75 gene
B
-ATc
+ATc
C
DIC
DAPI
CPN60
- ATC
+ ATc 72h
D
- ATC
+ ATc 72h
P
C
PDH-E2
Mito-E2
Mito-E2

Table 1

	Toc75	SignalP	PlasmoAP	PATS	Sam50	MitoProt	PlasMit
Toxoplasma gondii	**TGME49_072390*	N	N	N	*TGME49_205570*	N	N
Neospora caninum	*NCLIV_034910*	N	N	N	*NCLIV_020120*	N	Y
Eimeria falciformis	*EfaB_MINUS_25052.g2122*	N	N	N	NF	-	-
Eimeria praecox	*EPH_0025670*	Y	N	N	NF	-	-
Eimeria necatrix	*ENH_00027930*	N	N	n	*ENH_00075630*	N	N
Plasmodium falciparum	*PF3D7_1234600*	Y	Y	Y	**PFF0410w*	N	Y
Plasmodium_chabaudi	*PCHAS_145150*	N	Y	Y	*PCHAS_010750*	N	Y
Plasmodium_berghei	*PBANKA_144920*	N	Y	Y	*PBANKA_010690*	N	Y
Plasmodium_yoelii	*PY17X_1451700*	N	Y	Y	*PY17X_0108400*	N	Y
Plasmodium_cynomolgi	*PCYB_146020*	N	N	N	*PCYB_114820*	N	Y
Plasmodium_knowlesi	*PKH_145170*	Y	Y	N	*PKH_114100*	N	Y
Plasmodium_vivax	*PVX_100680*	Y	Y	Y	*PVX_113574*	N	N
Theileria_equi	NF	-	-	-	*BEWA_051860*	N	N
Babesia_bovis	NF	-	-	-	*BBOV_III000300*	N	N

* Newer gene model does not agree with our experimental data. See GeneBank accession numbers: TgToc75 KT271755, PfSam50 KT271756

Table S1

Localization	Name	GeneID	SignalP4.1						SignalP3.0					
			C-Score	Y-Score	S-Score	D-Score	SP?	AA at +1	C-Score	Y-Score	S-Score (max	D-Score	SP?	AA at +1
PPC	PPP1	TGME49_287270	0.11	0.115	0.207	0.123	NO		0.043	0.056	0.269	0.103	NO	
PPC	ATrx2	TGME49_310770	0.198	0.303	0.709	0.369	YES	A	0.299	0.449	0.985	0.665	YES	A
PPC	TgApicE2	TGME49_295990	0.356	0.251	0.405	0.224	NO		0.294	0.405	0.993	0.500	YES	S
PPC	CDC48AP	TGME49_321640	0.356	0.251	0.405	0.224	NO		0.288	0.410	0.944	0.433	YES	V
PPC	TgApicE1	TGME49_314890	0.353	0.188	0.133	0.143	NO		0.200	0.033	0.165	0.089	NO	
PPC	Ubiquitin	TGME49_223125	0.137	0.145	0.215	0.149	NO		0.105	0.085	0.498	0.155	NO	
PPC	UDF1AP	TGME49_285700	0.128	0.136	0.195	0.137	NO		0.067	0.064	0.371	0.100	NO	
outermostmembrane	FtsH	TGME49_259260	0.112	0.12	0.147	0.124	NO		0.087	0.042	0.177	0.069	NO	
outermostmembrane	TGME49_201270	TGME49_201270	0.111	0.106	0.111	0.102	NO		0.034	0.017	0.060	0.017	NO	
outermostmembrane	ATrx1	TGME49_312110	0.265	0.371	0.734	0.418	YES	V	0.370	0.490	0.890	0.468	YES	V
outermostmembrane	APT	TGME49_261070	0.108	0.105	0.157	0.101	NO		0.063	0.044	0.306	0.074	NO	
second inner-most	Toc75/Omp85	TGME49_272390	0.209	0.242	0.685	0.352	YES	V	0.444	0.326	0.993	0.453	YES	V
Innermost	Tic20	TGME49_255370	0.611	0.753	0.99	0.849	YES	Q	0.633	0.701	0.989	0.815	YES	T
Innermost	Tic22	TGME49_286050	0.694	0.58	0.691	0.519	YES	L	0.740	0.755	0.919	0.735	YES	L
luminal	PDH E1b	TGME49_272290	0.415	0.608	0.963	0.77	YES	S	0.539	0.442	0.967	0.653	YES	L
luminal	FabH	TGME49_231890	0.118	0.121	0.157	0.119	NO		0.072	0.073	0.409	0.124	NO	
luminal	PDH E2	TGME49_206610	0.524	0.662	0.961	0.754	YES	Q	0.599	0.625	0.961	0.740	YES	L
luminal	PGKII	TGME49_225990	0.129	0.15	0.279	0.149	NO		0.124	0.080	0.846	0.127	NO	
luminal	FabD	TGME49_225990	0.379	0.37	0.53	0.391	YES	P	0.532	0.530	0.885	0.586	YES	V
luminal	PDH E3	TGME49_305980	0.125	0.23	0.56	0.312	NO		0.127	0.192	0.924	0.495	YES	R
luminal	GyraseB	TGME49_297780	0.109	0.117	0.137	0.117	NO		0.030	0.039	0.310	0.130	NO	
luminal	GyraseA	TGME49_221330	0.609	0.693	0.956	0.763	YES	R	0.679	0.614	0.927	0.069	YES	R
luminal	FNR	TGME49_298990	0.198	0.262	0.641	0.321	NO		0.204	0.358	0.950	0.600	YES	V
luminal	ACP	TGME49_264080	0.47	0.629	0.929	0.744	YES	Y	0.628	0.678	0.970	0.715	YES	F
luminal	TGME49_239680	TGME49_239680	0.275	0.286	0.382	0.291	NO		0.647	0.379	0.985	0.525	YES	S
luminal	TPI-II	TGME49_233500	0.437	0.46	0.765	0.489	YES	F	0.236	0.320	0.913	0.401	YES	F
luminal	FabI	TGME49_251930	0.271	0.399	0.914	0.53	YES	F	0.470	0.402	0.974	0.522	YES	F
luminal	PYKII	TGME49_299070	0.12	0.112	0.132	0.114	NO		0.438	0.079	0.110	0.058	NO	
luminal	RP128	TGME49_209710	0.558	0.477	0.7	0.474	YES	F	0.937	0.707	0.958	0.753	YES	F
luminal	CPN60	TGME49_240600	0.139	0.192	0.349	0.224	NO		0.259	0.359	0.861	0.465	YES	F
luminal	ACC1	TGME49_221320	0.221	0.276	0.52	0.313	NO		0.533	0.446	0.748	0.493	YES	A
luminal	PDH Ea	TGME49_245670	0.128	0.151	0.254	0.148	NO		0.274	0.137	0.876	0.213	YES	P
luminal	ICDH2	TGME49_266760	0.822	0.736	0.892	0.699	YES	S	0.928	0.711	0.901	0.709	YES	R
luminal	YbaK	TGME49_255680	0.107	0.102	0.111	0.099	NO		0.027	0.022	0.072	0.039	NO	
luminal	UROD	TGME49_289940	0.116	0.114	0.163	0.111	NO		0.102	0.139	0.346	0.138	NO	
luminal	2-C-methyl-D-erythritol 2,4-cyclodiphosphate synthase domain-containing protein	TGME49_055690	0.503	0.653	0.944	0.654	YES	P	0.352	0.501	0.943	0.576	YES	S
luminal	Product: 1-deoxy-D-xylulose-5-phosphate synthase	TGME49_008820	0.11	0.107	0.13	0.106	NO		0.062	0.033	0.119	0.035	NO	
luminal	HU	TGME49_027970	0.235	0.468	0.968	0.72	YES	E	0.364	0.529	0.995	0.700	YES	E
luminal	LipB	TGME49_115640	0.14	0.145	0.34	0.192	NO		0.175	0.116	0.412	0.128	NO	
luminal	RNA helicase	TGME49_291670	0.387	0.497	0.95	0.678	YES	L	0.615	0.572	0.979	0.714	YES	V
luminal	hypothetical	TGME49_059230	0.708	0.556	0.712	0.467	YES	R	0.458	0.626	0.986	0.728	YES	H
luminal	hypothetical	TGME49_039320	0.112	0.132	0.207	0.143	NO		0.052	0.060	0.617	0.172	NO	
luminal	hypothetical	TGME49_039680	0.275	0.286	0.382	0.29	NO		0.647	0.379	0.985	0.525	YES	S
luminal	hypothetical	TGME49_002440	0.178	0.239	0.412	0.24	NO		0.126	0.296	0.947	0.391	YES	W
luminal	hypothetical	TGME49_001270	0.111	0.106	0.111	0.102	NO		0.034	0.017	0.060	0.017	NO	
luminal	NFU	TGME49_021920	0.148	0.222	0.482	0.218	NO		0.415	0.282	0.902	0.338	YES	H
luminal	DNAdDNAh	TGME49_008840	0.111	0.11	0.134	0.104	NO		0.055	0.054	0.527	0.291	NO	

Table S2 - primers used in this study

Primer name	Primer sequence	Purpose
TgToc75_EcoRI_F	CCGAATTCATGGCGGAGGAAGAAAGAC	Forward to amplify TgToc75^{78} for ectopic expression in *Toxoplasma*
TgToc75_78_NsiI_R	CCATGCATAGAAACTGGAGAAGACCC	Reverse to amplify TgToc75^{78} for ectopic expression in *Toxoplasma*
TgToc75_95_NsiI_R	CCATGCATAAGAGGGGCGGGGGTGC	Reverse to amplify TgToc75^{95} for ectopic expression in *Toxoplasma*
TgToc75_277_NsiI_R	CCATGCATTCACGATATCCACGAAGGTACG	Reverse to amplify TgToc75^{277} for ectopic expression in *Toxoplasma*
TgToc75_512_NsiI_R	CCATGCATAAACTGCGTCGTCTGTCGTCTG	Reverse to amplify TgToc75^{512} for ectopic expression in *Toxoplasma*
TgToc75_790_NsiI_R	CCATGCATAGCCTGCGAACGACGACGCCTC	Reverse to amplify TgToc75^{790} for ectopic expression in *Toxoplasma*
TgToc75_FL_NsiI_R	CCATGCATTGAAGCTGTTGTCGGCCACG	Reverse to amplify TgToc75$^{full\text{-}HA/Ty}$ for ectopic expression in *Toxoplasma*
TgSam50_EcoRI_F	CCGAATTCATGGCGGGGTCAGCTCC	Forward to amplify TgSam50$^{full\text{-}HA}$ for ectopic expression in *Toxoplasma*
TgSam50_NsiI_R	GGATGCATACTACTCGGGGAGTCTTCC	Forward to amplify TgSam50$^{full\text{-}HA}$ for ectopic expression in *Toxoplasma*
PfOToc75_X_F	AACTCGAGATGAAAAATGTTTTAAGAAAATATAC	Forward to amplify PfToc75^{78} for ectopic expression in *Plasmodium*
PfToc75_78_A_R	GGCCTAGGTCTTGTTGTTAGCTTATTCCATAATTC	Reverse to amplify PfToc75^{78} for ectopic expression in *Plasmodium*
PfSam50_X_F	CTCGAGATGTTTAATTATTTTTTAAGAAGC	Forward to amplify PfSam50^{N} for ectopic expression in *Plasmodium*
PfSam50_60_A_R	AACCTAGGTAAACAAAAATGCTTCCAAAATAATGG	Reverse to amplify PfSam50^{N} for ectopic expression in *Plasmodium*
PfOmp85_95_A_R	GGCCTAGGTCCTGTTTCTTCATTTTCTGTTTCC	Reverse to amplify PfToc^{95} for ectopic expression in *Plasmodium*
Toc75prorepcosf	GTATGCACATGTCTCTTTTCTGAATCTTTCGCATGAGAAG CAATGCTCCATCGAATGGTAACCGACAAACGCGTTC	Cosmid recombineering to create promoter replacement vector.
Toc75prorepcosr	AGTCCACGACTCAAAAGAGCGAAACGTGTGTTTCTACGGT CGCTCAACGTAGATCTGGTTGAAGACAGACGAAAGC	Cosmid recombineering to create promoter replacement vector.
toc75cosproinserf	ACGTTGAGCGACCGTAGAAACACACGTTTCGCTCTTTTGA GTCGTGGACTGAATGGTAACCGACAAACGCGTTC	Cosmid recombineering to create promoter insertion vector.
toc75cosprionsrev	ATTGAACACCGCCGCCGTGGCGACGATGCCTGTCTTTCTT CCTCCGCCATTTTAGATCTGGTTGAAGACAGACGAAAGC	Cosmid recombineering to create promoter insertion vector.
HA_NsiI_F	CCATGCATTACCCGTACGAC	Primer to amplify 3xHA tag
HA_PacI_R	GGTTAATTAATTAGAGCTCGGC	Primer to amplify 3xHA tag
Apg-qPCR-F	TCTATTGCAATGGAAAAAGGTATG	qPCR to score apicoplast genome
Apg-qPCR-R	TCAATGGTAGAGCAAAGGACTG	qPCR to score apicoplast genome
UPRT-qPCR-F	ACTGCGACGACATACTGGAGAAC	qPCR to score nuclear genome
UPRT-qPCR-R	AAGAAAACAAAGCGGAACAACAA	qPCR to score nuclear genome
ACP$_{F/A}$mutF	*CTGATCAGGCCTGGTGACACAGCACCGTAGGAAGAAGCAA TGG*	Mutagenesis of F at position +1 of ACP to A
ACP$_{F/A}$mutR	*CCATTGCTTCTTCCTACGGTGCTGTGTCACCAGGCCTGAT CAG*	Mutagenesis of F at position +1 of ACP to A
ACP$_{Y/A}$mutF	*CCTGGTGACACAAAACCGGCGGAAGAAGCAATGGATG*	Mutagenesis of Y at alternative position +1 of ACP to A
ACP$_{Y/A}$mutR	CAT*CCATTGCTTCTTCCGCCGGTTTTGTGTCACCAGG*	Mutagenesis of Y at alternative position +1 of ACP to A